DIGITALCOMMONS
—@WAYNESTATE—

Wayne State University

Wayne State University Theses

1-1-2015

Hiv Integrase Mechanisms Of Resistance To Raltegravir, Elvitegravir, And Dolutegravir

Kyla Nicole Ross
Wayne State University,

Follow this and additional works at: https://digitalcommons.wayne.edu/oa_theses

🎨 Part of the Biochemistry Commons, Bioinformatics Commons, and the Virology Commons

HIV INTEGRASE MECHANISMS OF RESISTANCE TO RALTEGRAVIR, ELVITEGRAVIR, AND DOLUTEGRAVIR

by

KYLA ROSS

THESIS

Submitted to the Graduate School

of Wayne State University,

Detroit, Michigan

in partial fulfillment of the requirements

for the degree of

MASTER OF SCIENCE

2015

MAJOR: BIOCHEMISTRY AND

MOLECULAR BIOLOGY

Approved By:

_____
Advisor   Date

DEDICATION

I dedicate this thesis to my late step brother Carlton Lowry.

ACKNOWLEDGEMENTS

I would like to thank everyone in the Kovari lab for their generous help with this thesis. I thank Ben for helping me with the manuscripts, the research, and the experiments and for being a great colleague and an awesome friend. I thank Brad for answering the most complicated questions, for suggesting alternative approaches, and for being a great friend. I thank Cathy for being there to listen, the awesome conversations and for being a great colleague. I would like to thank Tamaria for giving me this project and offering her professional input. I would like to thank Iulia for being an awesome life coach, for pushing me and listening to my issues when life got complicated. I would like to thank Dr. Kovari for having me in his laboratory, being an excellent mentor, advisor and teacher. I learned a lot about the scientific method while under his guidance. I would like to also thank Dr. Brian Edwards and Dr. Zhe Yang for being on my committee and for being excellent professors. I would also like to thank them for their suggestions and input on this thesis. I would also like to thank everyone in the BMB department.

I would also like to thank my family for being there for me at the toughest of times and for rooting me on through it all. I thank my parents Wanda and Howard, my sisters Kyra and Karmyn, my brothers Marcus, Markeith, and HJ, my aunt Dee Dee, my little cousin Niyah and my best friend Britney for being there to talk to me and for being positive no matter what was going on.

I would like to thank David West for being there for me throughout the entire graduate program. His positive advice and caring demeanor helped me though the hardest of times. Thank you for seeing me through so much.

TABLE OF CONTENTS

LIST OF TABLES

LIST OF FIGURES

CHAPTER 1 : INTRODUCTION

1.1 HUMAN IMMUNODEFICIENCY VIRUS TYPE 1

Human immunodeficiency virus type 1 (HIV-1) is a lentivirus retrovirus that utilizes CD^{4+} T cells to replicate. As a result of this phenomena, $CD4^+$ T cells no longer help with immunity; this leads to immune system failure and increased susceptibility to infections [1]. At this stage, the body cannot defend itself from foreign pathogens and succumbs to a HIV-1 related death [2]. Once the number of CD4+ cells drop below a certain quantity, the HIV-1 positive status will evolve into AIDS (Acquired Immune Deficiency Syndrome)[3].

HIV-1 can be acquired from an infected person by unprotected sexual intercourse, during birth, or by a blood transfusion [4–6]. The transition to AIDS can take up to 15 years. The unique genome and structure of the virus makes it one of the greatest current threats to human health [1, 3, 4].

1.2 HIV-1 EPIDEMIOLOGY

Since the discovery of AIDS in 1981, there has been a rapid decrease in the number of infections in developed countries but in less developed countries there are still millions of new infections every year (**Fig. 1-1**). In 1983, it was determined that HIV-1 was the instrumental agent of AIDS [1, 7]. As of 2013, there were about 35.0 million people reported to be living with HIV-1 internationally with 3.2 million being children under the age of 15, who reside mostly in low- to middle- income countries. In 2013, 71% of the 2.1 million newly infected patients resided in Sub-Saharan Africa [8].
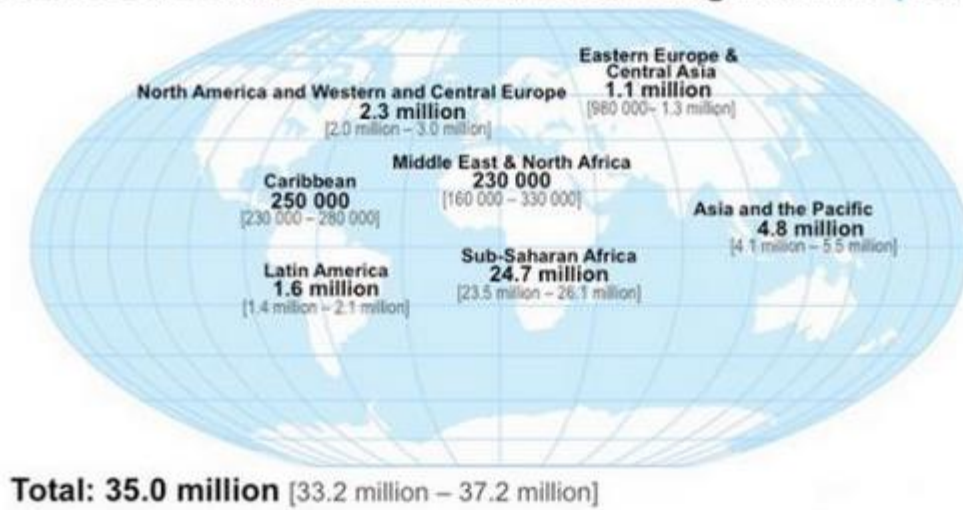
Figure 1-1: *An International Outlook on the HIV-1 Epidemic*. According to the World Health Organization, as of 2013, 35.0 million are infected with HIV-1, most of whom reside in Sub-Saharan Afric (Adapted from http://www.unaids.org/).

1.3 HIV-1 GENOME

The HIV-1 genome has genes that code for several structural proteins that are common to all the retroviruses; however, it also has over lapping and open reading frames for accessory regulatory proteins which make the HIV-1 genome unique [9].

The genes of the HIV-1 genome that code for structural proteins are the gag, pol, and env proteins (**Fig. 1-2**). The gag gene encodes the capsid proteins. The gag precursor encodes four viral structural proteins – matrix (p17), capsid (p24), nucleocapsid (p7) and p6 – which are processed by the mature viral protease. The gag- pol gene encodes three viral replicating proteins Integrase (IN), Protease (PR), and Reverse Transcriptase (RT). The env gene encodes the surface lipoproteins gp120 and gp41 [9, 10].

The essential regulatory elements of the HIV-1 genome are the tat and rev genes (**Fig 1-2**). The tat gene regulates the reverse transcription of the viral RNA. This gene is responsible for efficient synthesis of viral mRNAs and the regulation of the release of virions from infected cells. The rev gene stimulates the production of HIV-1 proteins and suppresses the expression of HIV-1 regulatory genes [9].

The accessory regulatory genes are the nef, vif, vpr, and vpu genes (**Fig. 1-2**). The nef gene encodes a protein that is located in the cell's cytoplasm that retards HIV-1 replication. The vif gene increases infectivity of HIV-1 particles and encourages the cell to degrade APOBEC3G (host cell protein that acts as an innate antiviral agent). The vpr gene accelerates the production of HIV-1 proteins and the vpu gene helps with the assembly of new virus particles, helps them to bud from the host cells and enhances the degradation of CD^{4+} proteins[9–12].
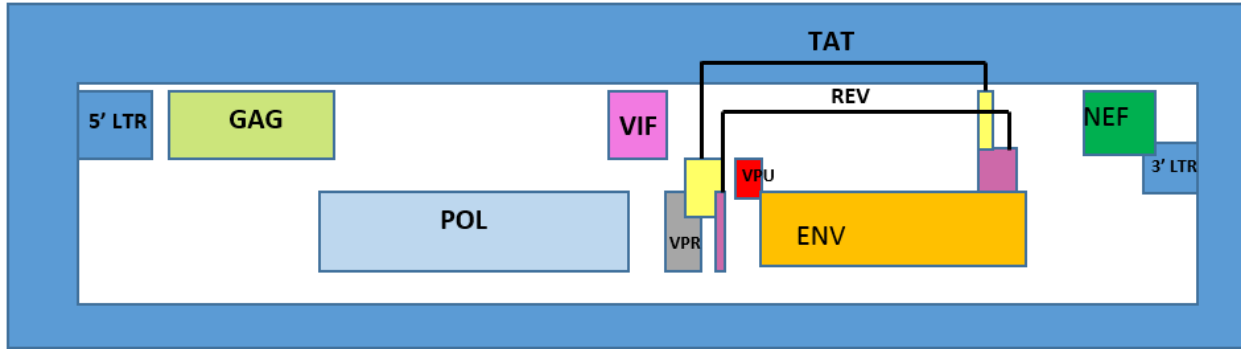
Figure 1-2: *The HIV-1 Genome.* The HIV-1 genome consist of genes that encode structural and replication proteins: gag(lime), pol (light blue), and env (orange) and regulatory proteins: vif (pink), tat(yellow), rev (purple), vpu (red), vpr (gray) and nef (green).

1.4 HIV-1 LIFE CYCLE

HIV-1 has a similar structure as many of the retroviruses. The outer coat is around 120 nm in diameter, roughly spherical and is composed of a lipid bilayer; this is known as the viral envelope (**Fig 1-3**). Embedded throughout the viral envelope are proteins from the host cell and 72 copies of the HIV-1 surface envelope proteins called Env (**Fig 1-3**). Env spikes through the surface of the viral envelope and consist of three glycoproteins and one hundred and twenty caps that are anchored by stems. Beneath the viral envelope lies an HIV-1 protein called p17 or the matrix. Past the matrix is the capsid formed by p24 proteins. Inside the capsid are non-covalently linked positive single stranded RNA strands and the replication enzymes RT and IN (**Fig.1- 3**)[13, 14].
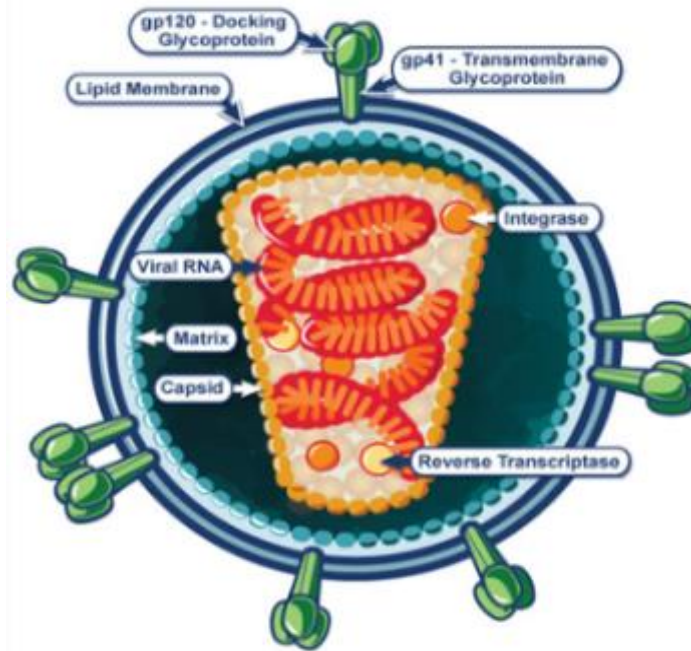
Figure 1-3: *The structure of HIV-1.* HIV-1 consists of a spherical lipid membrane that encloses a capsid which encloses its genetic information and replication proteins. On the surface of the protein, there are docking glycoproteins that are required for docking and fusion into lymphocytes. (Adapted from www.NIAID.gov).

The HIV-1 life cycle has multiple steps that make it a highly infective provirus. First, a free HIV-1 particle interacts with the surface of a CD^{4+} lymphocyte. The viral glycoproteins (g120 proteins) on the surface of the retrovirus bind to the CD^{4+} receptor and co-receptor on the surface of the host cell. Once bound, the membranes fuse together forming an opening. The virus releases a capsid containing two positive sense viral RNA strands, viral enzymes and viral core proteins into the cytoplasm of the host cell (**Fig.1- 3 and 1-4**). The capsid core proteins are degraded, and its contents are released into the cytoplasm. Reverse transcriptase takes the viral RNA strands and reverse transcribes them into viral DNA in the cytoplasm of the host cell (**Fig. 1-4**). Integrase integrates the viral DNA into the DNA of the infected cell by two mechanisms: 3' processing and stand transfer.

Once the infected cell is activated, the proviral DNA is transcribed into viral mRNA. The viral mRNA leaves the nucleus and enters the cytoplasm where a new virus is being synthesized. Some of the mRNA is translated into a polypeptide chain by a ribosome on the surface of the rough endoplasmic reticulum. The remaining viral proteins are assembled on the surface of the infected cell's membrane. Once this occurs, two mRNA strands and the polyprotein chain are aligned on the opposite side of the membrane of the glycoproteins on the surface of the infected cell. From here, the new viral particle buds out the infected cell. Inside this new particle, protease cleaves itself from this long polyprotein and it begins to cleave the remainder of the chain, forming the matrix, the capsid, RT and IN establishing a mature virion (**Fig. 1- 4**) (review in ref. [15]).
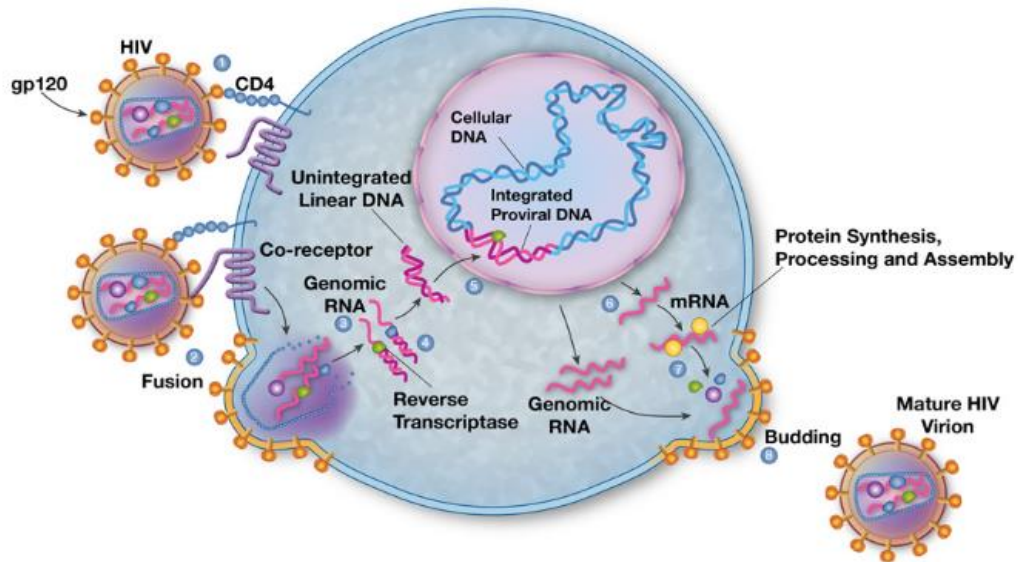
Figure 1-4: *HIV-1 replication cycle.* **HIV-1 using CD4+ T- cells to replicate.** The process begins when a free HIV-1 virion attaches to the surface of the CD4+ cell and causes a fusion which result in the insertion of its viral genome. From here, the genome is reversed transcribed, integrated, and forms a new virion. The virion is not mature until the viral protease cleaves itself from the newly translated polyprotein and proceeds to cleave and form proteins that are required for the replication cycle. (Adapted from www.drcin.com).

1.5 STANDARD CARE

As of late 2012, there has been a 30% decrease in AIDS related deaths due to highly active antiretroviral therapy (HAART) [16]. Major risk factors for death by AIDS include a viral load that is greater than 400 copies/ mL and a CD^{4+} T cell count less than 200 cells/mL [16]. HAART subdues HIV-1 replication. This antiviral therapy consists of three drugs that target separate stages of the HIV-1 life cycle: 2 nucleotide reverse transcriptase inhibitors, a non-nucleotide reverse transcriptase inhibitor, integrase inhibitor, or protease inhibitor [17–19]. HAART provides treatment options for both naive and experienced patients. The treatment can decrease plasma concentrations of viral RNA to undetectable levels, increase amounts of $CD4^{+}$ T cells, and decrease the occurrence of HIV-1 related diseases (such as cancer) and excess mortality [16].

Though HAART decreases the viral load below detectable levels, it does not eradicate the virus entirely due to viral latency and antiretroviral resistance. Post integration HIV-1 latency is a proviral complex that forms in resting $CD4^{+}$ T cells. $CD4^{+}$ T cells that form this complex go undetected by the immune system [20]. Once these cells are activated by recall antigens or cytokines, the proviral complex can produce a virus that is able to replicate efficiently [21]. Although rare, HIV-1 viral latency is established during an acute infection (a few days after exposure) [22]. Viral resistance also makes it impossible to eradicate HIV-1 entirely. HAART uses drugs that target different stages in the viral life cycle and the replication enzymes. The replication enzymes develop genetic mutational pathways that result in resistance to the inhibitor thus allowing the proteins to evade treatment. Over time, the enzyme will completely resist the inhibitor but continue to aid in the replication process. [23][24][25][26]. In order to keep these complications under control, the various HAART regimens must last for the patient's lifetime [16][18].

1.6 HIV-1 REPLICATION PROTEINS

There are three enzymes that are required for HIV-1 replication to be effective: reverse transcriptase (RT), integrase (IN), and protease (PR). The functions of these enzymes makes them major protagonist in HIV-1 infection. RT produces a complimentary DNA strand from the viral RNA template; IN integrates the viral genome into the host cell's genome; and PR generates key counterparts for maturing virus particles that enable them to continue the replication process [27, 28], [29].

1.7 HIV-1 INTEGRASE

HIV-1 IN inserts reverse transcribed viral DNA (vDNA) into the host cell genome. It is encoded by the end of the pol gene of the HIV-1 genome and functions as a multimeric protein [30, 31]. The 288 residues (32 kDa) of HIV-1 IN form three functional domains: the N- terminus domain, the catalytic core domain (CCD) and the C- terminus domain (Fig. 1-3)[31]. The N-terminus domain (residues 1-49) contain an HHCC motif that binds Zn^{2+}; this "zinc finger" homologue stabilizes the protein's quaternary structure (Fig.1-3) [32–35]. The catalytic core domain (residues 50-212) contains a $DD_{35}E$ motif (the catalytic triad) that coordinates two Mg^{2+} cofactors in the presence of its substrate. In the apoprotein, one Mg^{2+} is coordinated between D116 and D64. Once the vDNA is present, a second Mg^{2+} is coordinated between D64 and E152 [36, 37]. Molecular dynamics experiments and crystallographic studies have revealed a flexible surface loop conformation that enters the active site during IN's reaction with vDNA [38, 39]. This loop is named the 140's loop because it consists of residues 138-152 [38, 40]. These residues participate in catlysis and substrate binding reactions making it a vital part of IN's enzymatic activties [40–43]. The C- terminal domain (residues 213- 288) interacts both specifically and nonspecifically

with vDNA ensuring stability of the HIV-1 IN and vDNA (IN•vDNA) complex throughout

catalysis (**Fig. 1-5**) [31],[37],[44]
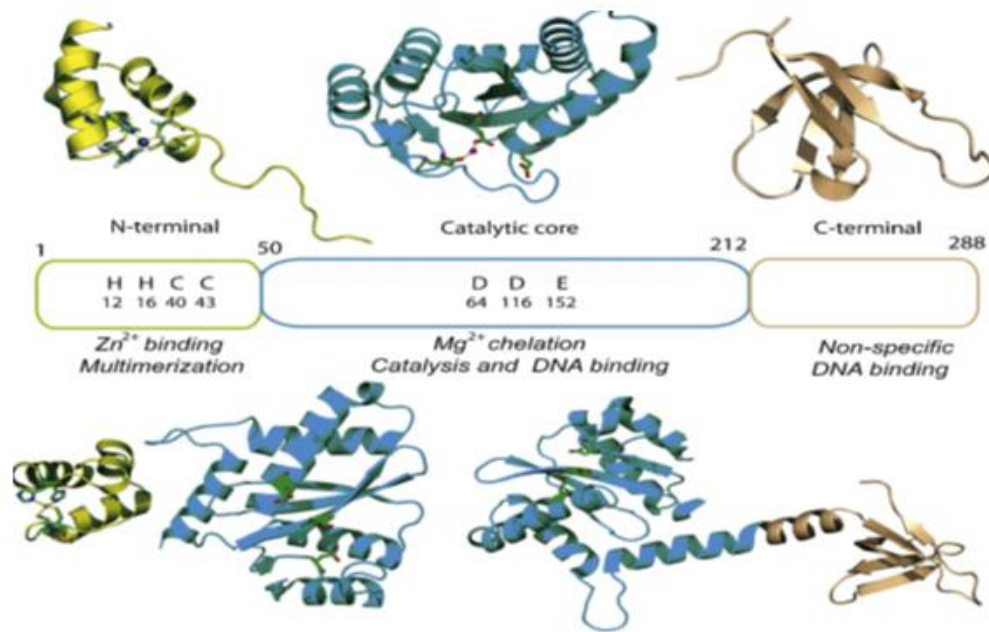
Figure 1-5: *The structure of HIV-1 IN.* HIV-1 IN consists of 3 functional domains termed the N-terminus domain (NTD), the catalytic core domain (CCD) and the C- terminus domain (CTD). All three domains have been crystallized in pairs or truncated, but there is no crystal structure of the protein as an entity. (Adapted from Delelis *et al*., 2008)

1.7.1 HIV-1 IN MECHANISMS OF CATALYSIS

IN generates the proviral status of HIV-1 by catalyzing 3' processing and strand transfer (**Fig. 1-6**) [45–48].

In the cytoplasm of an infected cell, after the viral RNA is reverse transcribed into viral cDNA (vDNA), the autonomous 3' processing reaction begins (**Fig.1-6a and b**). During 3' processing, dimeric IN specifically binds to the U3 and U5 regions of the long terminal repeats (LTR) of the vDNA (adjacent to a conserved CA dinucleotide) and catalyzes an endonucleolytic cleavage reaction resulting in the release a dinucleotide and the exposure of reactive 3' hydroxyl groups [31][45, 49, 50].

After 3' processing, the recombinant IN and vDNA complex (IN•vDNA) forms the pre-integration complex (PIC), a 61 Å diameter complex that includes other viral and intracellular proteins and aids in nuclear transport [15]. Once the PIC is in the nucleus, the strand transfer process begins [51–53],[54].

Strand transfer is the mechanism where IN covalently inserts vDNA in to the hDNA (host DNA) (**Fig. 1-6c and d**). IN (in its dimer of dimers conformation) disrupts the phosphodiester bonds of the hDNA via nucleophilic attack by the reactive 3'hydroxyl groups of the 3' ends of the vDNA [2, 20, 21]. This reaction occurs simultaneously with 5 base pairs between the two points of insertion indicating that the reactive hydroxyl groups attack the hDNA at its major grooves [28, 31, 55, 56]·[15].

After stand transfer, the product consists of a 5' overhang and 5 base pair gaps (**Fig. 1-6e**). The 5' dinucleotide overhangs (resultant of the 3' processing mechanism) are cleaved and the 5 base pair gaps near the points of insertion are filled by cellular enzymes [31, 46]. *In vitro* studies have found that HIV-1 IN in the core catalytic domain catalyzes a disintegration mechanism which is the opposite reaction of strand transfer where the viral DNA is released from the host cell

genome [57–59]. It is suggested that IN performs the disintegration mechanism to facilitate the cleavage of the 5' overhang, a step which is required for integration of vDNA to be complete [46]. Although this has been observed *in vitro*, it has not been proven to take place *in vivo* [31].
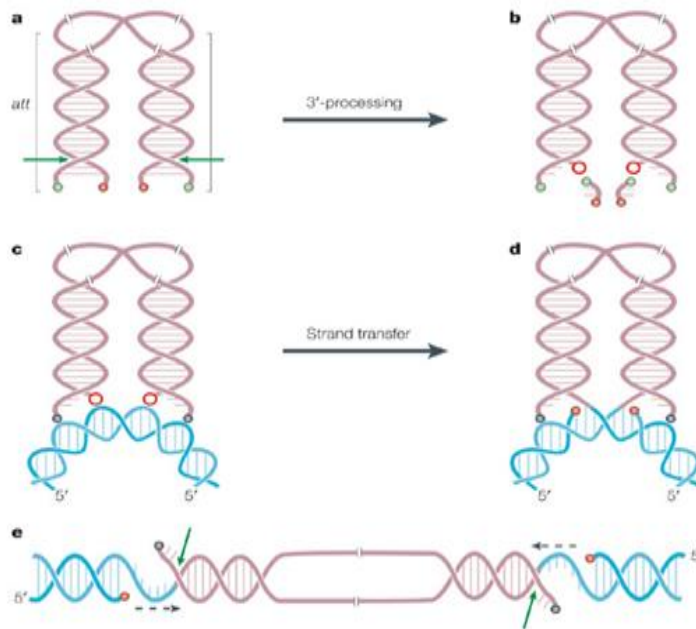
Figure 1-6: *HIV-1 IN catalytic activities*. HIV-1 IN catalyzes two autonomous reactions: 3' processing and strand transfer. During the 3' processing reaction, IN catalyzes an endonucleotyic cleavage of the 3' ends of the reverse transcribed vDNA in the cytosol. During the strand transfer reaction, IN covalently inserts vDNA in hDNA via nucleophilic attack. (Adapted from Delelis *et al*., 2008)

1.7.2 THE PRE- INTEGRATION COMPLEX

The formation of the PIC complex is essential for efficient viral replication; it ensures that integration of the viral genome is successful. PIC formation starts with the reverse transcriptase (RT) complex. Throughout the early steps of the life cycle, RT, IN, vDNA, and other viral and cellular proteins are a part of a larger complex. After RT transcribes vRNA (viral RNA) into vDNA, it is degraded from the assembly as it approaches the nucleus via the actin network and and PIC is formed. PIC aids in the translocalization of IN•vDNA into the nucleus [15, 60, 61].

1.7.2.1 IN•VDNA COMPLEX DURING 3'PROCESING AND STRAND TRANSFER

Because the full length structure of HIV-1 IN has not been determined due to IN's interdomain flexibility and high insolubility, the prototype foamy virus integrase (PFV IN) homology model and many biochemical assays have been used to model the complete structure of the IN•vDNA complex. Based on crystal structures of PFV IN in complex with vDNA and also *in vitro* studies performed on the full length HIV-1 IN, the substrate pocket has been proposed to consist of all three functional domains; the whole enzyme in its dimer and multimeric form is required for substrate binding (**Fig. 1-7**) [62, 63]. Monomer-1 (IN1) and monomer-2 (IN2) bind the U5 and U3 LTR in the hDNA, respectively. Monomer 1' (IN1') and monomer 2' (IN2') domains are required for stability during the catalytic mechanisms (**Fig. 1-7**).
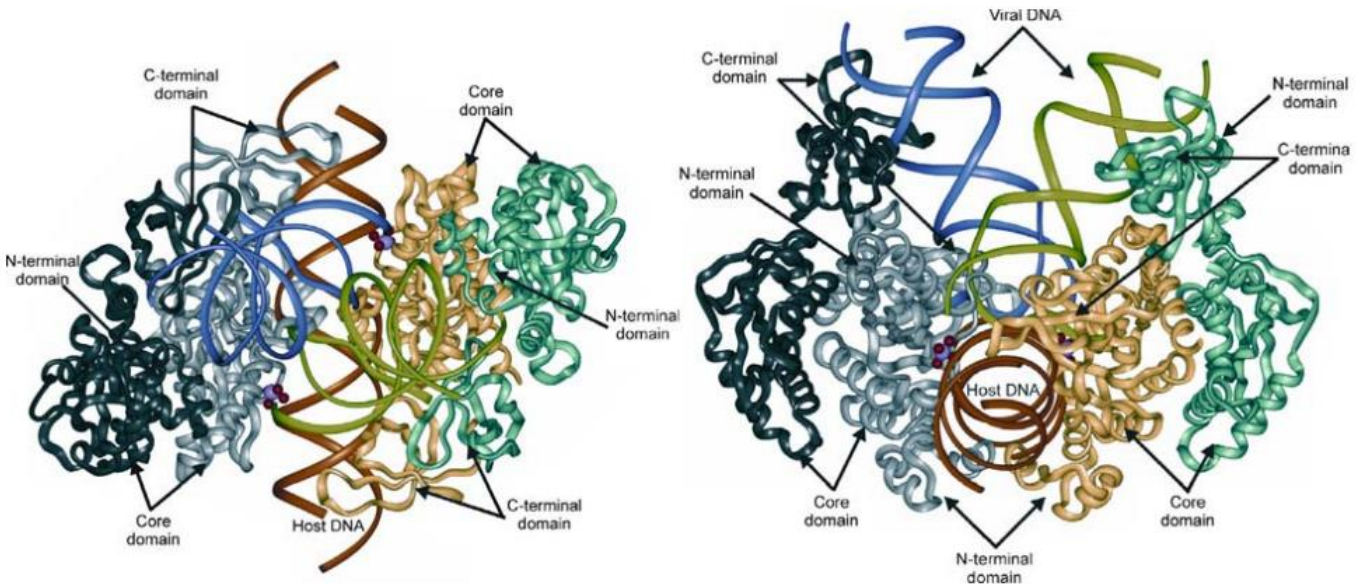
Figure 1-7: *HIV-1 IN binding to vDNA.* The 3D model of HIV-1 IN in complex with vDNA by Dolan *et al.* suggest that IN1 (gray) active site is used to insert the U5 LTR 3' end (green) into the hDNA (orange) and IN1' (black) promotes stability during the reaction. IN2 (orange) active site is used to insert the U3 LTR 3' end (blue) into the hDNA and IN2' (green) promotes stability for this process. (Adapted from Dolan *et al.,* 2009)

During the 3' processing reaction, IN makes specific and nonspecific interactions with its vDNA substrate. IN interacts with the heterocyclic bases of codon A17. This interaction destabilizes the interaction between nucleotide 17 and 18 (thymine 18 and adenosine 17). The destabilization results in a high 3` processing rate. Base pairs at positions 8-11 have been shown to be important for 3' processing. Residues 186-193 make up a flexible loop conformation that is located near the C-terminal end of the CCD. These residues bind specifically with the minor groove of the vDNA at positions 8- 11. Residues 246- 250 of IN1 and residue 20 of IN2 interact with the backbone of position 8'- 11'. These specific interactions consist of basic residues in the C-terminus and the phosphodiester backbone of the vDNA's LTR. Residues 256- 264 in the C-terminal domain of IN2 nonspecifically interact with the bases at position 3' and 4'. Residues R262, R263, K244, G247, Q53, and V54 of IN 2 interact with the phosphodiester backbone of nucleotides at position 5-7. These interactions with base pairs 3-7 are nonspecific and only promote stability among the complex during catalysis [62, 64, 65].

IN makes specific and nonspecific interactions with viral DNA during strand transfer. When IN is in its multimeric form, the LTR of the vDNA and acceptor hDNA interact with two adjacent subunits (monomer 1 (IN1) inserts U5 and monomer 2 (IN2) inserts U3). The interactions between IN and the LTRs of U3 and U5 mirror one another. IN binds specifically to the LTR- LTR junction of the vDNA via residues 143, 148, 156, 159, 160, 230, 246, 262, 263, and 264; these residues have been observed in molecular models to be near the six base pairs of the LTR and the ends of the processed vDNA 3' [56, 62, 64, 66]. A17 is within hydrogen bonding distance of the Mg^{2+} and its phosphate group forms hydrogen bonds with N155, K159 and T66. C16 is in the active site, adjacent to K156 and its carbonyl group points towards Q148 of the 140s loop. K156's side chain forms hydrophobic interactions with the deoxyribose ring of C16 and it also interacts

with G4`. G4` forms specific interactions with Q148 via is carbonyl group; this interaction would account for IN active site's specificity for this base pair. T3` is flipped out by Q146 of the active of IN1 causing it to interact specifically with Q53 and N144 in IN2 [56, 62, 64, 66].

Throughout the strand transfer reaction, the 140s loop acts as a plough, keeping the U5 and U3 vDNA ends separated. This separation is due to the 5 base pair gap generated by insertion of the vDNA into the hDNA [56, 62, 64]. When the 140s loop residues are altered in ways that decrease mobility of the loop, viral activity is decreased substantially [40, 66].

The preferred region of insertion for IN on the hDNA is typically an area where the phosophodiester backbone is bent and slightly unwound along its major groove. Residues S119, N120, C130, W132, and K159, (located along the cleft of the dimer IN) have been reported to interact with hDNA during the strand transfer reaction. IN binding is mediated through the phosphodiester backbone of hDNA that is wrapped around nucleosomes [54, 62, 64].

1.7.2.2 PROTEIN- PROTEIN INTERACTIONS

For HIV-1 IN activity to be efficient, the pre-integration complex must contain cellular and viral proteins that stabilize IN and stimulate its activity.. Investigators have found that PIC complexes are karyophilic; host cell proteins direct PIC complexes through the nuclear pore (reviewed in ref. [15]). The viral proteins that take part of the PIC are IN (in complex with donor vDNA and highly karophilic), matrix proteins (regulates integration), Vpr (mediates the nuclear import of PICs in slowly or non-dividing cells, and stimulates transcription of viral LTRs and regulates cellular apoptosis [15, 61, 67].

Host cell proteins that have been identified as part of the PIC are as follows: barrier-to-autointegration factor (BAF) protects vDNA from autointegration and stimulates intermolecular recombination when target DNA is located; survival motor neuron–interacting protein 1 (Gemin2) stimulates reverse transcription and nuclear import of the PIC; cellular acetyltransferase (p300)

acetylates IN and controls its activity; the nonhistone chromosomal protein HMG I(Y) brings the vDNA ends together in the active site and acts as a sensor for regulatory input of vDNA during strand transfer; chaperonin hHSP 60 stimulates IN activity and protects IN from denaturation; WD- 40 repeat protein human EED plays a role in intracellular and nuclear transport; importin 7 (imp7) contributes to nuclear import and reverse transcription; transcriptional activator integrase interactor 1 (INI1) which stimulates integration and targets vDNA to active genes, lens-epithelium- derived growth factor(LEDGF-p75) tethers IN to chromatin, protects it from denaturation and stimulates integration; uracil DNA glycosylase (UDG) participates in nuclear translocation of the PIC [68–78].

1.7.3 HIV-1 IN INHIBITORS

Integrase inhibitors (INIs) decrease the replication rate of HIV-1 RNA by effectively disrupting mechanisms that IN performs during the HIV-1 life cycle. INIs have either been classified as strand transfer inhibitors (INSTIs) or allosteric inhibitors (NCINIs) [79],[80].

Since there is no full length structure of IN interacting with INSTIs, various biochemical assays have been performed to determine the mechanism of action, binding modes, and therapeutic index of INSTIs [37, 81]

INSTIs consist of planar diketo acid (DKA) derived bioisoteric scaffolds that chelate the active site Mg^{2+} and a hydrophobic component that interacts with side chains of residues and vDNA in a ternary binding pocket that competes with the binding of vDNA (**Fig. 1-8**) [80][81] . The DKA moiety analogues enable the INSTI to compete with vDNA for the catalytic binding pocket and the halogenated hydrophobic component increases specificity and affinity of the inhibitors target protein [37, 80–82]. The chelating hydroxyl groups of the DKA analogues chelate the Mg2+ ions. The binding of INSTIs halobenzyl ring (the hydrophobic component) via Van der

Waals interactions in the pocket of the active site where vDNA adenosine (A17) resides displaces the vDNA and stabilizes the molecule, therefore disengaging the IN•vDNA complex [37, 80, 83]. The vDNA is then circularized by cellular enzymes and persists in the nucleus for an undetermined duration[37].

The proposed binding site for INSTIs is based on INSTI resistance profiles. INSTIs bind to IN only if the vDNA is present in the active site during the assembly of the PIC; after 3' processing but before strand transfer [37, 80, 81]. Due to these mechanisms of action and binding, INSTIs are considered "metal dependent" compounds and "interfacial inhibitors" [37, 82].

INSTIs have a resilient time- of- drug addition profile; these compounds have been observed to increase the formation of cDNA and hence decrease integration. Mutations have been found in drug resistant INs; and, *in vitro*, mutated viruses treated with an INSTI have been shown to be inactive, which explains the high therapeutic index of INSTIs for IN [37].

Currently there are three HIV-1 inhibitors (INIs) approved by the Food and Drug Administration (FDA): Raltegravir (RAL), elvitegravir (ELV), and dolutegravir (DTG). All three INIs are considered integrase strand transfer inhibitors (INSTIs) due to their specific inhibition of the stand transfer process [84–86].

1.7.3.1 FDA APPROVED HIV-1 INTEGRASE STRAND TRANSFER INHIBITORS
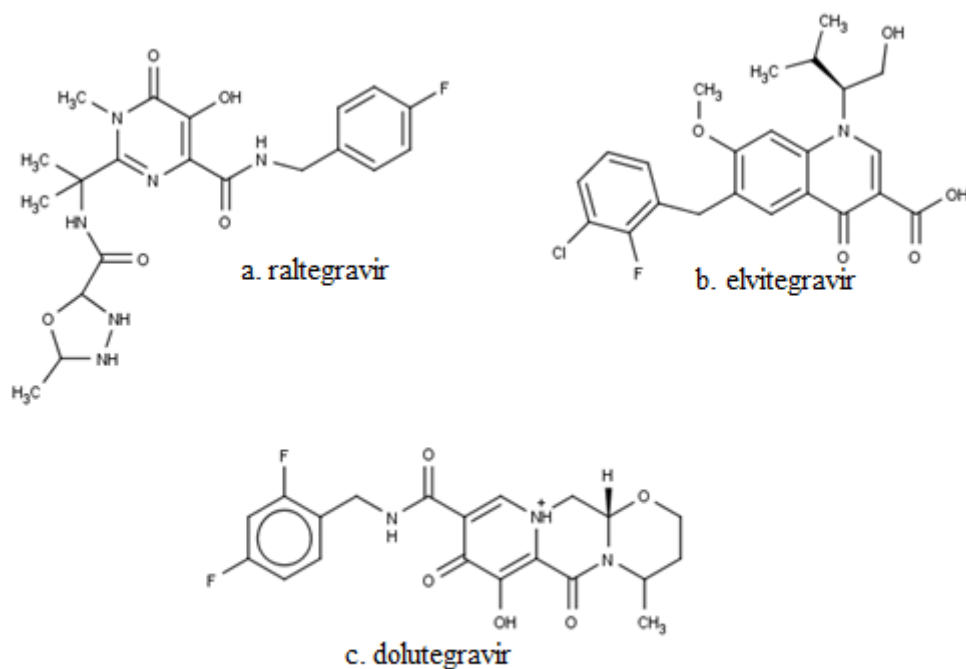
Figure 1-8: *FDA approved INSTIs.* The FDA has approved three INTIs for commercial usage: a: Raltegravir (RAL), b: Elvitagravir (ELV), and. c: Dolutetravir (DTG). The pharmacophores encircled in green are protruding scaffolds from RAL (oxadiazole ring) and ELV (1-hyrdroxymethyl2- methylpropyl group) DKA core; blue are the halobenzyl groups of each INSTI; and red are the DKA analogues and the chelating oxygen atoms.

1.7.3.2 RALTEGRAVIR

On October 7, 2007, raltegravir (RAL) became the first INSTI to be approved by the Food and Drug Administration. RAL was developed by Merck and Co. under the generic name Insentress; the patent expires October 3, 2023 [87],[88].

RAL has a hydropyrimidone that acts as RAL's DKA analogue and a carboximide side chain that acts as the heteroatomic feature. RAL's oxadiazole ring makes a ∏ stacking connection with Y143 and P145 [42],[58],[89]. RAL's halogenated benzyl ring extends into the tight pocket created by the A17 nucleotide of the vDNA[90].

1.7.3.3 ELVITEGRAVIR

Elvitegravir (ELV)) is a cobicistat boosted INI that is administered in a quad pill formulation with the RT inhibitors tenofovir and emtricitabine called Stribild [91]. Stribild was developed by Gilead Sciences, which licensed the inhibitor from Japan Tobacco in 2008. Elvitegravir was approved by the Food and Drug Administration on August 27, 2012 and its patent expires in 2029 [92, 93].

ELV has a quinolone-3- carboxylic group which serves as a substitution for the DKA moiety and a carboxylic/ β- ketone scaffold that serves as the chelating heteroatoms [94]. ELV's 1-hydromethyl-2-methylpropyl groups serves as a substitution for RAL's oxadiazole ring which interacts with Y143 and P145 via Van der Waals interactions [90, 95]. ELV also contains a linker that connects the DKA bioisoteric component to its flurobenzyl ring that interacts with E152 and vDNA [43, 56, 94].

1.7.3.4 DOLUTEGRAVIR

Dolutegravir (DTG) is a second generation INI that was approved by the Food and Drug Administration on August 12, 2013. DTG (formerly known as S/GSK1349572) was developed by

ViiV Healthcare and is known by the generic name Tivicay [96],[97]. The patent expires October 5, 2027 [97]. DTG is considered a second generation INI due to its ability to retain activity against viral strains that result in viral resistance to RAL and ELV *in vitro.* It is the first unboosted INSTI on the market[98–100].

DTG has a tricyclic carbomoyl pyridine DKA analogue that contains three coplanar oxygen atoms which act as the chelating agents [98]. DTG's hydrophobic component is a diflourophenyl ring which is attached to an extended flexible linker that occupies the tight pocket near the active site. This diflourophenyl ring interacts with carbon atoms of the catalytic residues E152 and Q148 via Van der Waals contacts. This extended linker region digs deeper into the tight evacuated pocket enabling DTG to make more intimate interactions with the vDNA. It has the ability to adjust its position and conformation when there is a structural change in IN's active site. DTG's tricyclic chelating core extends toward G118. DTG spans the full width of the active site but only spans half of its height. [41, 43].

1.7.3.5 CABOTEGRAVIR (GSK1265744)

Cabotegravir (CAB) is similar to DTG with a carbamoyl pyridine DKA analogue and diflourophenyl pharmacophores [101, 102]. Administration of CAB is different from all of the existing INIs on the market. While it is administered orally, it is also being tested as a monthly intramuscular injection that includes the NNRTI TMC278-LA [103]. ViiV Healthecare has run eight phase 1 and phase 2 trails to determine the pharmacokinetic parameters of CAB; they administered a two-drug regimen every 4 to 8 weeks via an intramuscular injection (800 mg) and oral (30 mg) formulations of CAB and rilpivirine (a non-nucleoside inhibitor) [103].

1.7.3.5 NON - CATALYTIC INTEGRASE INHIBITORS

1.7.3.5.2 BI-224436

Another INI currently in clinical trials is BI-224436 which was developed by Boehringer Ingelheim [104]. BI-224436 (BI2) disrupts the interactions between IN and LEDGF/p75 protein by binding to the allosteric binding pocket, which is located in the CCD dimer interphase at residues A124, T125, A128, E170, and H171; it is the first NCINI to go into clinical trials [63, 105].[106].

BI2 has 3 substituents that provide metabolic stability (C4), potency (C7) and binding (C3 and C4). The core pharmacophore of BI2 is a C4 moiety that consists of a hybridized chromane and quinolone arene system which provides potency and metabolic stability; C3 consists of an alkoxyl group that fills the hydrophobic pocket and provides favorable binding affinity and increased potency; C7 is connected to a hydrogen which enables potency serum shifts [106].

1.7.4 ANTIRETROVIRAL ACTIVITY

1.7.4.1 RAL RESISTANCE

Major mutation pathways that are associated with IN resistance to RAL are [Q148H/K/R] ± [G140S/A] and {E138K/A}, [N155H]±[E92Q], and [Y143C/R]± [T97A] [107–110]. Primary mutations Q148H/R/K decreases IN susceptibility to RAL by 5- to 50- fold whereas the double mutant Q148H/R/K and G140S/A reduces susceptibility by more than 100- fold; E138K/A is selected in combination with the primary mutation Q148H [111]. These genetic pathways have been associated with therapeutic failure. This decreased potency has been shown to result in near WT viral loads [111–114]. The mutation Y143C/R reduces susceptibility to RAL when selected alone [109]. When the double mutant Y143C/T97A is selected, IN susceptibility to RAL is reduced by more than 100-fold [109, 115]. [N155H] has been associated with RAL failure in patients because it restores viral activity to near WT levels [114].

1.7.4.2 ELV RESISTANCE

The mutational pathways that are associated with the highest level of resistance to ELV are the primary mutants [Q148H/K/R] ± [G140S/A], [N155H]±[E92Q], and [T66I/A/K] ± [S147G] [115–117]. According to *in vitro* and *in vivo* studies, the primary mutations Q148H/R/K, just as with RAL, reduce susceptibility to ELV and are associated with therapeutic failure [118, 119]. [T66A/I/K] is a primary mutation that was observed to be selected by IN when under ELV pressure in preclinical trials. An *in vivo* study done on patients that had previously failed treatment with ELV, mutation [N155H] was observed to be selected within the first two weeks of the study (*n*=5 out of 16) [120].

1.7.4.3 DOLUTEGRAVIR RESISTANCE

Just as with RAL and EVG, IN mutates in response to treatment with this second generation inhibitor. but the mutations produce minimal viral resistance. According to the Stanford HIV-1 Drug Resistance Database, codons 92,138,140, and 148 acquire mutations that are responsible for IN resistance against DTG [115, 117].If the primary mutant Q148H/R/K and accessory mutants G140S/A and E138K/A are alone, there is no clinically significant reduction in susceptibility to DTG [54]. In vitro, IN has been shown to select the primary R263K mutation along with H51Y, M50I, and E138K as secondary mutations [106, 107].

Table 1-1: HIV-1 integrase resistance mutations

	M50	H51	T66	E92	T97	E138	G140	Y143	S147	Q148	N155	R263
RAL				Q	A	A/K	S/A	R/H/C		H/R/ K	H	
ELV			I/A/ K	Q	A				G	H/R/ K	H	
DTG	I	Y				A/K	S/A			H		K

CHAPTER 2 : MATERIALS AND METHODS

2.1 HIV-1 INTEGRASE CATALYTIC CORE DOMAIN SYSTEM PREPARATION FOR MOLECULAR DYNAMICS SIMULATION

The WT catalytic core domain of HIV-1 IN was obtained from the Protein Data Bank (PDB: 1BL3). Chain C of 1BL3.pdb was used to construct homology models for the following mutants: [Q148H], [Q148H/G140S], [Q148R], [Q148H/G140S], [Q148R/G140A], and [N155H/E92Q]. The coordinates from the original PDB model (1BL3) and the new models were merged together to obtain crystallographic waters in the new models [42, 121].

The IN structure requires Mg^{2+} metal ions in the active site (coordinated between the DDE motif). 1BL3 contained only one Mg^{2+} ion in the active site (coordinated between D64 and D116); therefore, the PFV IN crystal structure (PDB: 3OYA) was superimposed with the models to incorporate the other Mg^{2+} ion between residues D64 and E152 [42, 90].

Models of the INSTIs RAL, ELV, and DTG were obtained from the Zinc Database (http://zinc.docking.org/). Each INSTI was submitted to Paramchem (https://cgenff.paramchem.org) for the generation of topology files and parameter files [122].

In order to properly coordinate the INSTIs RLT, ELV and DTG into the integrase active site, homologous structures containing the three inhibitors were obtained. The coordinates from the PFV IN complexed with RAL (PDB: 3OYA), ELV (PDB: 3L2U) and DTG (PDB: 3S3M) were used to manually dock the inhibitors into the active site of the CCD using the VMD TK console [41, 56, 90, 121]. The system was placed in a TIP3P water box (dimensions: 70x72x70 Å) and was neutralized with $MgCl_2$ [121].

2.2 ENERGY MINIMIZATION AND MOLECULAR DYNAMICS SIMULATIONS

Energy minimization of the systems was accomplished using the conjugant gradient method. The initial temperature of the system was set at 70K followed by an increase to 310K in 5K time steps [42, 123].

All of the MD simulations were performed with NAMD 2.9 for 40ns utilizing the CHARMM36 force field. Van der Waals (vdW) interactions were cut off at a 12Å distance. Long range electrostatic interactions were calculated using the Particle-Mesh Ewald (PME) method. Equations of motion were incorporated with a 2fs time step [123, 124].

The conserved NPT (model, pressure and temperature) ensemble was used to perform the simulations. To keep the system at a constant temperature of 310K, Langevin dynamics were used (the Langevin damping coefficient was set at $5ps^{-1}$) and the Nose- Hoover Langevin piston method was used to keep the pressure of the systems constant at 1atm [124, 125]. Twelve processors were used from the WSU high performance scientific computing GRID (**www.grid.wayne.edu**) to enable the MD simulations to run in parallel.

2.3 ANALYSIS

The molecular dynamics trajectory was loaded into VMD [121]. The VMD suite's timeline tool was used to calculate the RMSD of each Cα atom for the last 5ns of the simulation.

2.4 FULL LENGTH HIV-1 INTEGRASE SYSTEM PREPARATION FOR MOLECULAR DYNAMICS SIMULATION

The full length HIV-1 integrase structure has not been successfully crystallized and solved. Therefore, the full length HIV-1 integrase model was generated based on the crystal structure of the prototype foamy virus (PFV) structure (pdb: 3OYA). The full length HIV-1 integrase sequence was submitted to the Swiss-Model server using chain A of the PFV structure (pdb: 3OYA) as a

template [126, 127]. PFV has the same active site conformation with the DDE motif aiding in catalysis and functional domains as HIV-1 IN making it a suitable template (**Fig. 2-1**). The previously published integrase structures for the CCD (pdb: 1BL3), NTD, plus CCD (pdb: 1K6Y), and CTD plus CCD (pdb: 1EX4) domains were then superposed onto the SwissModel structure. The linker regions generated from the SwissModel server were merged with the known crystallographic structures to generate our full length HIV-1 integrase model. After generation of the full length model, each system was prepared for simulation as previously described [42].
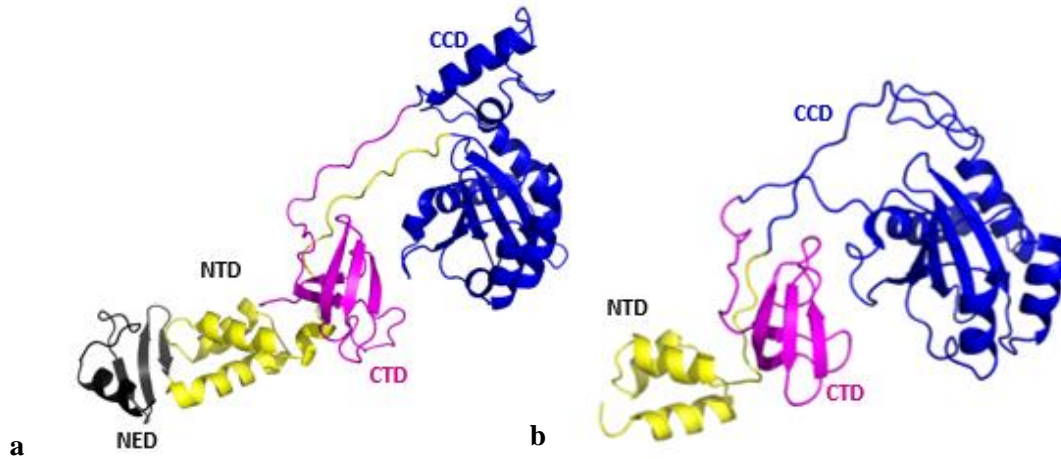
Figure 2-1: *Full length HIV-1 integrase modeled from PFV integrase*. (a). Prototype foamy virus integrase from PDB 3OYA with the CCD shown in blue, CTD shown in magenta, NTD shown in yellow and NED shown in dark grey. (b). Full length model of HIV-1 integrase with same color scheme for each domain. The HIV-1 IN model was built from the CCD structure (1BL3), NTD and CCD structure 1K6Y, and the CTD and CCD structure (1EX4).

2.5 ANALYSIS

The last 5ns of the trajectory was loaded into VMD 1.9.2. Then, for each simulation the backbone RMSD of each residue was calculated using the timeline tool with the first frame post energy minimization acting as a reference. The Ramachandran analysis tool was used to analyze the φ and ψ angles of the 140s loop residues over the duration of the trajectory. The depicted residues are those that showed significant φ and ψ angle differences to what was observed in our prior work [42].

Interactions between the ligand, viral DNA and protein were quantified to determine differences in molecular recognition. LigPlot+ version 1.4.5 and Nucplot v.1.0 were used to analyze INSTI-protein and viral DNA-INSTI interactions, respectively [128] [129]. The number of interactions were measured every 2000th frame of the 20,000 frame simulation and were averaged over the resulting ten frames.

CHAPTER 3 : REDUCED HIV-1 INTEGRASE FLEXIBILITY CORRELATES WITH RALTEGRAVIR, ELVITEGRAVIR AND DOLUTEGRAVIR DRUG RESISTANCE

3.1. INTRODUCTION

HIV-1 integrase (HIV-1 IN or IN) is a multimeric enzyme that integrates the HIV-1 genome into the DNA of infected CD4+ T-cells. HIV-1 IN is encoded by the end of the *pol* gene [37, 47]. This 288 amino acid enzyme (32 kD) consists of three functional domains: the N-terminal domain (NTD), catalytic core domain (CCD), and C-terminal domain (CTD). The CCD has a catalytic triad (D64, D116, and E152) that coordinates two Mg^{2+} and a flexible catalytic loop (140s loop) that is required for activity [40, 130]. HIV-1 IN catalyzes two autonomous reactions termed 3'-processing and strand transfer. 3'processing involves endonucleolytic cleavage of the 3' ends of the viral DNA by dimeric IN resulting in the exposure of reactive hydroxyl groups [130]. Strand transfer mediates the covalent insertion of viral DNA into the host cell DNA through a transesterification reaction using the reactive hydroxyls produced via 3' processing as nucleophiles [31, 51, 53].

Currently there are three HIV-1 IN inhibitors (INIs) approved by the Food and Drug Administration (FDA) for clinical use: raltegravir (RAL), elvitegravir (ELV), and dolutegravir (DTG). All three drugs function as strand transfer inhibitors (INSTIs) [37, 80–83, 131] and have a planar diketo acid (DKA) derived bioisoteric scaffold that chelates the active site Mg^{2+} and a halogenated hydrophobic component in the form of a halobenzyl group that increases specificity and affinity (**Fig 1-8 and Fig. 3-1**) [80, 82, 95, 132].
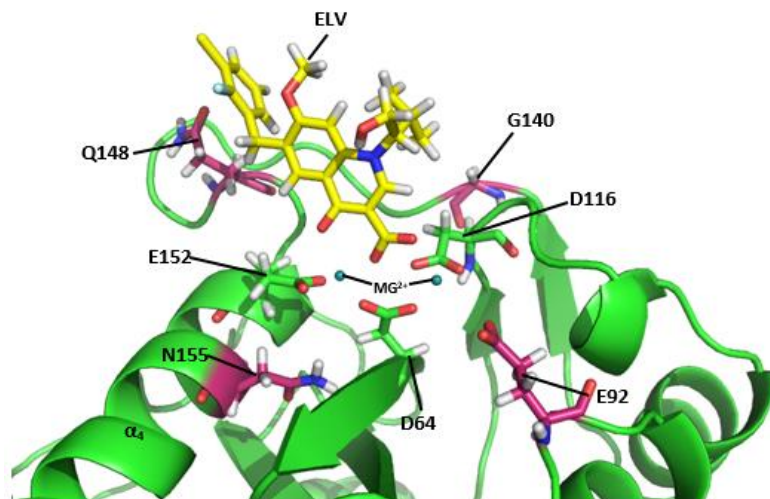
Figure 3-1: *HIV-1 integrase (PDB: 1BL3) active site in complex with elvitegravir*. Elvitegravir (ELV) diketo acid motif chelates the active site Mg2+ in HIV-1 IN's active site**.** ELV is shown as yellow sticks, Mg^{2+} are shown as blue spheres, the IN catalytic triad is shown as sticks, and the drug resistance mutations are shown as purple sticks.

According to the Stanford HIV Drug Resistance Data Base (http://hivdb.stanford.edu) RAL and ELV share a cross resistance profile. The mutations that IN acquires when challenged with RAL or ELV include the single mutants [Q148H] and [Q148R] and the double mutants [N155H/E92Q], [Q148H/G140S], and [Q148R/G140A] [112, 115, 118, 133]. These mutation pathways decrease IN susceptibility to RAL and ELV and increase therapeutic failure [31, 41, 43, 111–114, 118, 134–140] . In our previous work, we studied the protein flexibility and secondary structural alterations that occurred in the CCD domain of WT HIV-1 IN [Q148H/R] and [Q148H/R, G140S/A], in a 10 ns molecular dynamics simulation when bound to RAL [42]. We found that the mutants displayed a decreased flexibility relative to the WT model. We also discovered that the 140s loop in each mutant adopted a rigid hairpin conformation that functioned as a gate and decreased the RAL residency time [42]. To further investigate these findings, we ran a 40 ns molecular dynamics simulation on the IN CCD of WT, [Q148H/R], [Q148H/R, G140S/A] and [N155H, E92Q] as apoproteins and in complex with RAL, ELV, and DTG to investigate a) the effect that these mutations have on protein flexibility, b) how IN flexibility affects INSTI complexes and c) to determine if there is a relationship between IN flexibility and INSTI resistance. A decrease in flexibility is observed in the apoprotein mutants relative to the apoprotein WT. The mutant forms of IN that display the most resistance in viral susceptibility studies display high RMSD values in the 140s loop region relative to their corresponding WT-INSTI complex. These findings suggest that the conformational changes that occur in these mutants decrease the flexibility of the CCD which changes the shape of the active site. When this occurs, IN-INSTI complex interactions are weakened, ultimately causing drug resistance.

3.2 RESULTS

To investigate the effects that [Q148H], [Q148R], [Q148H, G140S], [Q148R, G140A] and [N155H, E92Q] mutations had on the flexibility of the CCD of HIV-1 IN, the RMSD of each residue in each structure was calculated. Calculations were derived from the last 5 ns of a 40 ns simulation of the CCD as an apoprotein and also in complex with RAL, ELV, and DTG. From these data, the effect that [Q148H/R], [Q148H/R, G140S/A] and [N155H, E92Q] had on HIV-1 IN CCD flexibility and the relationship between IN flexibility and INSTI resistance was identified. According to the results, the drug resistance mutations produced a less flexible apoprotein CCD relative to the WT apoprotein. As result, the 140s loop becomes more flexible in versions of mutant IN that display a higher level of resistance in reported *in vitro* work. This suggest that INSTIs binding mode to the 140s loop is altered as a result of the active site structural change.

3.4.1 MUTATIONS [Q148H], [Q148H, G140S], [Q148R], [Q148R, G140A] AND [N155H, E92Q] INCREASE THE RIGIDITY OF THE HIV-1 INTEGRASE PROTEIN

As shown in **Fig. 3-2**, the apoprotein IN mutants are less flexible than apoprotein WT IN. Also, in **Table 2**, the 140s loop is less flexible in the mutants that in WT IN.. These results suggest that conformational changes that occur is in the CCD changes the shape of the active site.
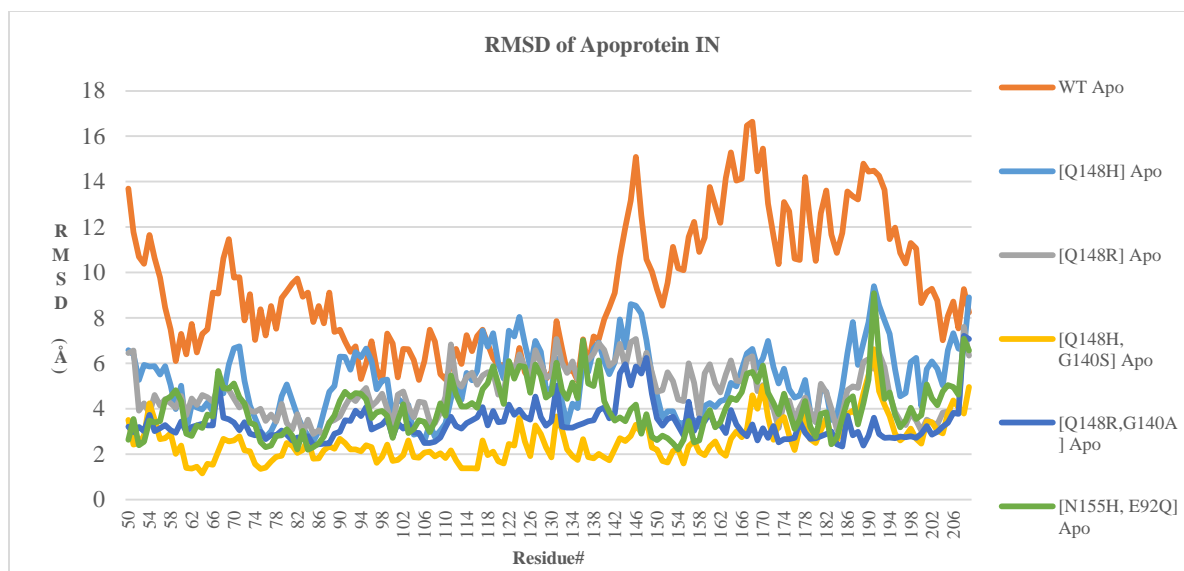
Figure 3-2: *Flexibility (RMSD) of the apoprotein HIV-1 integrase models.* The VMD suite timeline tool was used to calculate the root mean square deviation of Cα (RMSD) in each residue. The apoprotein IN displays the most flexibility relative to the various mutants.

Table 3-1: The RMSD of the 140s loop of apoprotein wild type and mutant HIV-1 integrase

Mutants studied	140s loop RMSD
WT	9.30Å
Q148H	5.27Å
Q148H, G140S	4.72Å
Q148R	2.58Å
Q148R, G140A	3.35Å
N155H, E92Q	4.05Å

Note: The average root mean square deviation (RMSD) values for each complex was used as an indicator of HIV-1 integrase flexibility. The mutant HIV-1 integrase are less flexible than the wild type HIV-1 integrase.

3.4.2 HIV-1 INTEGRASE STAND TRANSFER INHIBITOR RESISTANCE CORRELATES WITH THE FLEXIBILITY OF THE 140S LOOP

To investigate the relationship between IN flexibility and INSTI resistance, the RMSD of the 140s loop in each mutant in complex with RAL, ELV, and DTG were calculated (**Fig. 3-3a-d**). Results indicate that the 140s loop is more flexible in IN mutants that display the highest reported EC_{50} FC (fold change). These findings suggest that increased rigidity of the mutants reduces INSTI binding to the 140s loop.

The conformational changes in the CCD caused by drug resistant mutations resulted in increased flexibility of the 140s loop when in complex with RAL; this observation is indicated by increased flexibility of the 140s loop in mutants relative to WT RAL complexes (**Fig. 3b**). As presented in **Table 3**, all mutations display an increased EC_{50} FC value and higher 140s loop RMSDs when under RAL pressure relative to the WT- RAL complex (**Table 3**). This is an indicator of weakened interactions between RAL and IN.

The increased rigidity of the CCD caused by mutations increases the flexibility of the 140s loop in the CCD-ELV complexes. In **Table 3**, EC50 FC and RMSD values are highest in the [Q148H, G140S], [Q148R] and [Q148R, G140A] ELV complexes relative to the WT ELV complex (**Fig. 3-3c**). These mutants display a correlation between flexibility and resistance (**Table 3**).

When complexed with DTG, the mutants that exceed the WT EC_{50} display increased flexibility in the 140s region (**Table 3**). As presented in **Fig. 3-3d**, [Q148H] and [Q148R] in complex with DTG display decreased flexibility relative to WT-DTG because of the structural changes. In **Table 3,** [Q148H, G140S] and [N155H, E92Q] in complex with DTG display the highest EC_{50} FC values and an increased RMSD in the 140s loop relative to the WT DTG complex.

The effect of [Q148R, G140A] on IN susceptibility to DTG has not been studied *in vitro,* however, the 140s loop in this mutant is the most flexible. These data indicates a relationship between HIV-1 IN flexibility and resistance.

a.

b.
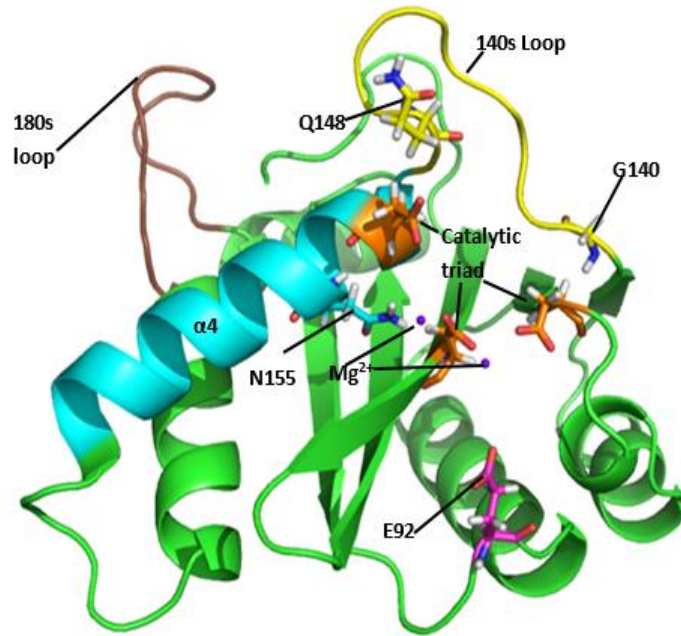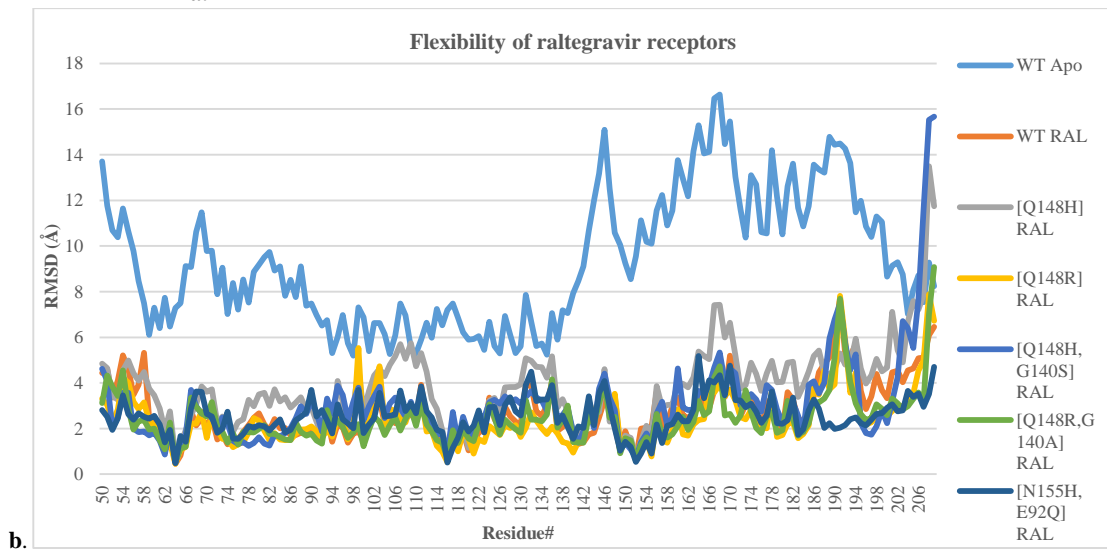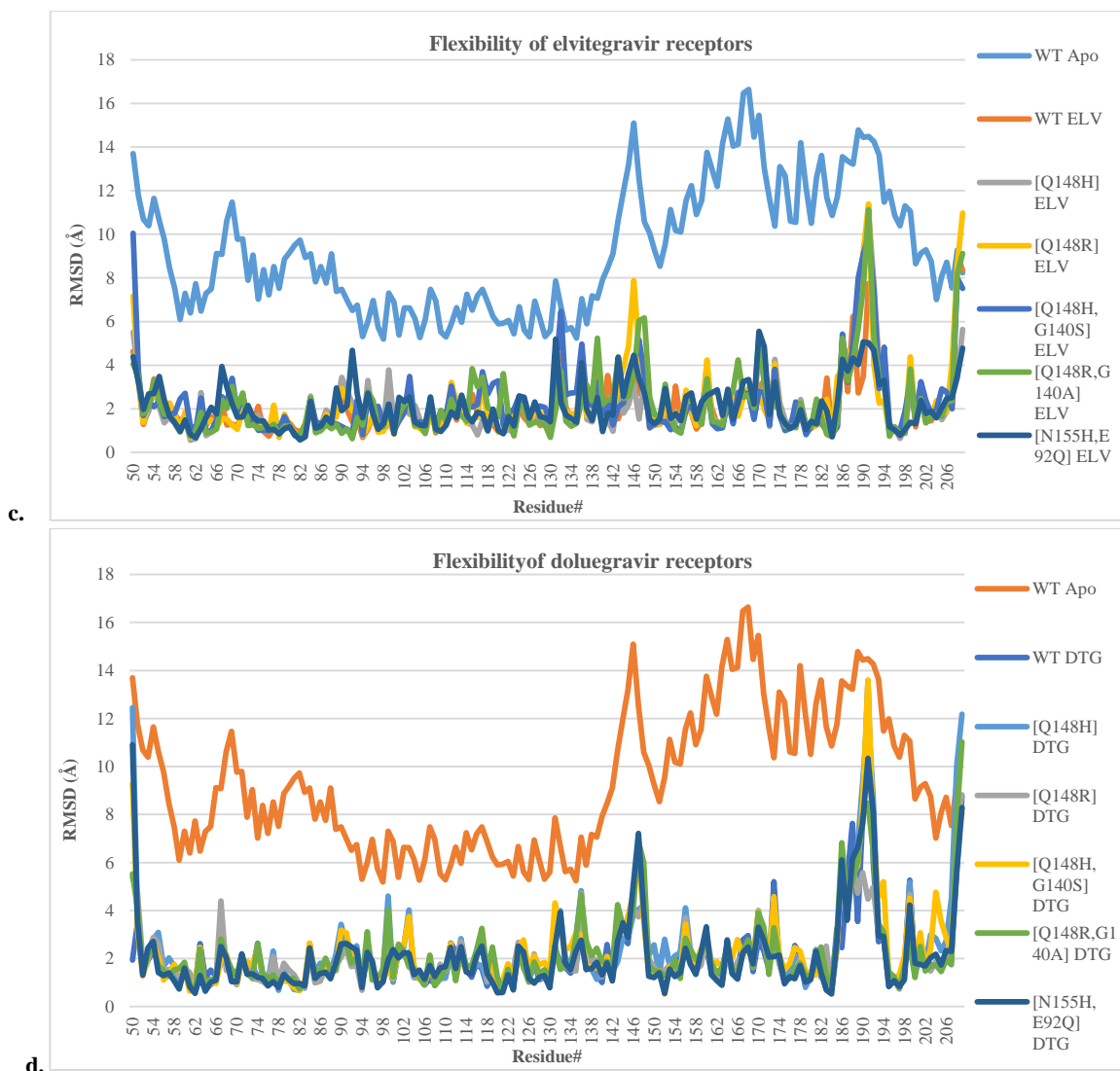
Figure 3-3a-d*: Flexibility (RMSD) of HIV-1 integrase mutants in complex with raltegravir, elvitegravir, and dolutegravir.* a) HIV-1 IN catalytic core domain outlining the catalytic triad (highlighted in orange) and the locations of the mutations (E92Q is highlighted in purple, the 140s loop is highlighted in yellow and α4 is highlighted in cyan). The plots in figure 3-3 display b) root mean square deviation of Cα (RMSD) of the wild type and mutant IN raltegravir complexes, c) the RMSD of the wild type and mutant IN elvitegravir complexes; and d) the RMSD of the wild type and mutant IN dolutegravir complexes. The yellow box enclose the 140s loop.

Table 3-2: Reported EC$_{50}$ fold change (EC50 mutant/ EC50 wild type ratio) *in vitro* data

Mutants	Raltegravir EC$_{50}$ (fold change)	Elvitegravir EC$_{50}$ (fold change)	Dolutegravir EC$_{50}$ (fold change)	140s loop RMSD in RAL complexes (Å)	140s loop RMSD in ELV complexes (Å)	140s loop RMSD in DTG complexes (Å)
WT	1.0	1.0	1.0	1.94Å	2.50Å	3.08Å
Q148H	13±5.0 [113]	7.3±2.3 [113]	0.97±0.090 [113]	2.58Å	1.92Å	2.65Å
Q148H_G140S	>130 [113]	>890 [113]	2.6±1.4 [113]	2.53Å	2.69Å	3.10Å
Q148R	47±9.3 [113]	240±91 [113]	1.2±0.21 [113]	2.41Å	3.41Å	2.85Å
Q148R_G140A	>100 [112]	>350 [112]	No data	2.19Å	3.58Å	3.47Å
N155H_E92Q	>130 [113]	320±39 [113]	2.5±1.2 [113]	2.49Å	2.50Å	3.07Å

*Note: These fold changes in EC$_{50}$ values (ratio: EC$_{50}$ of mutants/EC$_{50}$ of wild type) are derived from reported *in vitro* studies and correlate positively with our RMSD data. EC$_{50}$ fold changes for dolutegravir were substantially lower than both raltegravir and elvitegravir in the presence of mutations that typically lead to therapeutic failure [112, 113].

3.3 DISCUSSION

3.3.1 VIRAL ENZYME FLEXIBILITY AND DRUG RESISTANCE

Protein flexibility has been implicated in HIV-1 protease and HIV-1 IN resistance [95, 133, 141, 142]. IN flexibility (especially for the 140s loop) has been shown to be important for catalysis as well [40, 66, 130, 143]. Previously we found that the IN mutants [Q148H/R] and [Q148H/R, G140S/A] produce rigidity in the CCD when in complex with RAL. In this study, we observed the effects various drug resistance mutations had on CCD flexibility and the correlation between our molecular dynamics simulation results and reported experimental results. IN takes on a rigid conformation when the mutations are introduced. As a result of the structural alterations, IN's 140s loop flexibility is increased in the mutants that display the highest EC_{50} FCs in table 2.

The highest RMSD peaks in the models are in the 180s loop region (residue 185-195) (**Fig. 3-3a**). The 180s loop interacts with the minor groove of viral DNA during catalysis; the spike in RMSD is expected due to the absence of DNA in this study.

3.3.2 DOLUTEGRAVIR RETAINS EFFICACY AGAINST DRUG RESISTANT VIRUS

DTG showed the least sensitivity to the drug resistance mutations studied. The mutant IN DTG complexes RMSD deviated the least from the WT DTG complex. DTG also displayed the lowest EC_{50} FCs in the reported *in vitro* data (**Fig. 3-3d**). This is due to DTG's structural features. DTG contains the same active pharmacophores as RAL and ELV but structural differences enable DTG to have a prolonged residency time. DTG contains an extended linker that anchors its halobenzyl component deeper into the donor DNA's pocket in the active site and makes more vdW interactions with the backbone of the catalytic residue E152 causing increased rigidity of the active site (**Fig. 1-8** and **Fig. 3-3b**) [41]. Also, DTG's flexible structure gives it the ability to change its conformation with the active site of mutant HIV-1 IN, prolonging its residency time. These

features makes DTG less vulnerable to being pushed out of the active site in the resistant strains of IN.

3.3.3 IN SILICO METHODOLOGY AND DESIGN OF HIV-1 INTEGRASE INHIBITORS THAT RETAIN EFFICACY AGAINST THE DRUG RESISTANT VIRUS

The correlation between our *in silico* results and the in *vitro* reports show that this methodology can be a useful drug design and screening tool. New experimental inhibitors should show WT like binding patterns for mutant IN, which, in our studies, has shown minimal resistance. With this approach, INSTIs could be modified prior to synthesis to promote more rigidity of the 140s loop, minimizing the chance of drug resistance.

To further investigate the mechanism of drug resistance, we studied structural changes in HIV-1IN mutants [Q148H], [Q148H, G140S], [Q148R], [Q148R, G140A], and [N155H, E92Q]. In particular, changes in the HIV-1 IN 140s loop were examined. We then investigated the relationship between IN flexibility and drug resistance. Our findings suggest: a) the mutations cause IN flexibility to decrease, b) mutant INSTI complexes have increased 140s loop flexibility relative to the WT-INSTI complexes, and c) increased 140s loop flexibility in mutants correlates with higher *in vitro* EC50 fold change reported earlier.

CHAPTER 4 : REDUCED FLEXIBILITY OF FULL LENGTH HIV-1 INTEGRASE CORRELATES WITH DRUG RESISTANCE TO RALTEGRAVIR, ELVITEGRAVIR, AND DOLUTEGRAVIR

4.1 INTRODUCTION

HIV-1 integrase (IN) is a 32 kD multimeric enzyme that integrates the HIV genome into the DNA of infected CD4+ T-cells [37, 47]. IN contains three functional domains: the N-terminal domain (NTD), catalytic core domain (CCD), and the C-terminal domain (CTD) (**Fig. 1a**). The CCD contains the catalytic triad (residues D64, D116, and E152) that coordinates divalent metal ion cofactors (Mg^{2+}, Mn^{2+}), and a flexible catalytic loop (140s loop) which plays a major role in IN activity [40, 130] (**Fig. 1b**). IN catalyzes two autonomous reactions: 3' processing and strand transfer. 3' processing is the endonucleolytic cleavage of the viral DNA 3' ends by IN resulting in the exposure of reactive hydroxyl groups [130]. Strand transfer mediates the covalent insertion of viral DNA into the host cell DNA through a transesterification reaction using the reactive hydroxyl groups as nucleophiles [31, 51, 53].

Currently there are three HIV-1 IN inhibitors (INIs) approved by the U.S. Food and Drug Administration (FDA): raltegravir (RAL), elvitegravir (ELV), and dolutegravir (DTG). These inhibitors function as strand transfer inhibitors (INSTIs) [37, 80–83, 131]. INSTIs consist of a planar diketo acid (DKA) derived bioisosteric scaffold that chelates the active site Mg^{2+} ions, and a halogenated hydrophobic component that increases specificity and affinity for the IN active site (**Fig. 1b; Fig. 2**) [80, 82, 95, 132].
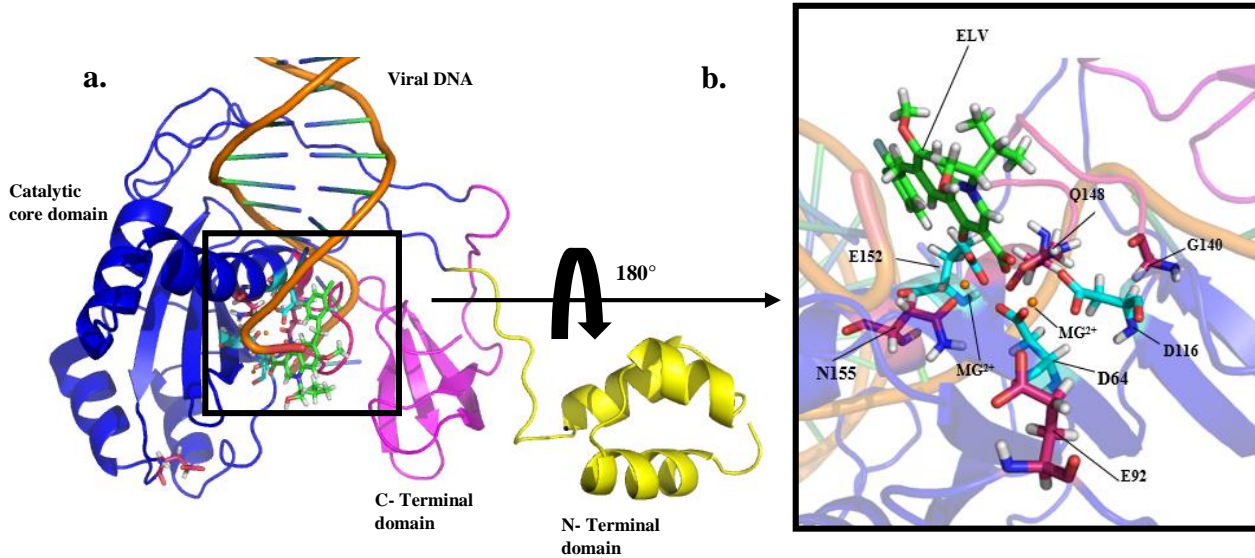
Figure 4-1: HIV-1 INTEGRASE HOMOLOGY MODEL AND ACTIVE SITE IN COMPLEX WITH ELVITEGRAVIR. The full length HIV-1 IN homology model was used to study secondary structural and molecular recognition differences between mutant and WT complexes. **(a)** The ternary complex consisting of viral DNA, the full length homology model which includes the n-terminal domain (yellow), the c- terminal domain (magenta), and the catalytic core domain (blue), and a INSTI. **(b).** The active site of the full length homology model showing ELV (green sticks) bound, ; Mg^{2+} are shown as orange spheres, the catalytic triad is shown in cyan sticks, and the mutant residues are shown in magenta sticks.

According to the Stanford HIV Drug Resistance Database [144, 145], RAL and ELV share a cross resistance profile. IN acquires several resistance mutations under RAL and ELV treatment pressure including the single mutants [Q148H] and [Q148R] and the double mutants [N155H/E92Q], [Q148H/G140S], and [Q148R/G140A] [112, 115, 118, 133]. These mutations decrease IN susceptibility to RAL and ELV and increase viral activity, ultimately leading to therapeutic failure [31, 41, 43, 111–114, 118, 134–140].

40 ns molecular dynamics (MD) simulations with the full length WT IN and the [Q148H/R], [Q148H/R, G140S/A] and [N155H, E92Q] IN drug resistant mutants as binary (protein and viral DNA) and ternary (protein, viral DNA, and INSTI) complexes were performed to investigate the following: a) the effect of these mutations on protein flexibility, b) secondary structural changes produced in the 140s loop, and c) the effect of these mutations on molecular recognition of the ligand by the protein and substrate. The mutant models displayed reduced flexibility, alternative 140s loop secondary structure conformations, and altered molecular recognition patterns compared to the wild-type model. These findings suggest that the decreased flexibility of the enzyme causes conformational changes in the active site of the mutants that may result in decreased INSTI binding affinity and residence time.

4.2 RESULTS

Mutations at position 92, 140, 148, and 155 cause decreased flexibility of HIV-1 IN. Our previous work reported decreased flexibility of the [Q148H], [Q148H, G140S], [Q148R], and [Q148R, G140A] CCD IN mutants in complex with RAL relative to the WT-RAL complex [42]. To examine whether these results could be reproduced with the full length model, we performed 40 ns simulations on binary complexes (protein and viral DNA) of WT and the mutants ([Q148H], [Q148H, G140S], [Q148R], [Q148R, G140A] and [N155H, E92Q]).

4.2.1 MUTATIONS DECREASE FLEXIBILITY OF HIV- 1 INTEGRASE

Mutations at position 92, 140, 148, and 155 cause decreased flexibility of HIV-1 IN. Previous work with the CCD IN reported decreased flexibility of the [Q148H], [Q148H, G140S], [Q148R], and [Q148R, G140A] mutant IN- RAL relative to the WT-RAL complex [42]. To examine whether these results could be reproduced with the full length model, we performed 40 ns simulations on binary complexes (protein and viral DNA) of WT IN and the mutants ([Q148H], [Q148H, G140S], [Q148R], [Q148R, G140A] and [N155H, E92Q]).

The binary mutant IN-RAL complexes displayed decreased flexibility relative to the WT-RAL complex as shown in **Fig. 4**. The average RMSD of the WT, [Q148H], [Q148H, G140S], [Q148R], [Q148R, G140A] and [N155H, E92Q] complexes are 5.88 Å, 2.29 Å, 2.43 Å, 1.98 Å, 1.97 Å, and 2.10 Å, respectively. (**Fig. 4**).
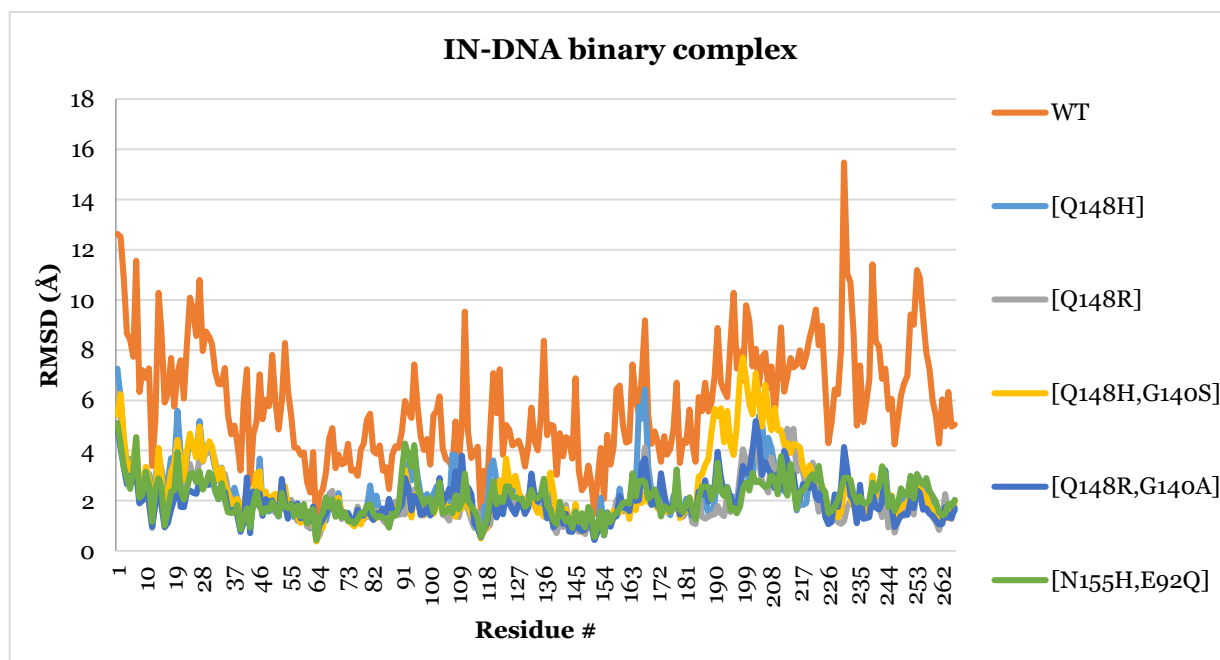
Figure 4-2: Resistance mutations reduce the flexibility of the IN-DNA binary complexes. The VMD suite timeline tool was used to calculate the root meant square deviation of Cα (RMSD) for each residue in the binary mutant and WT complexes. This approach analyzed the effects that mutants had on HIV-1 IN flexibility. The mutant HIV-1 IN structures are more rigid than WT IN.

4.2.2 CHANGES IN 140S LOOP SECONDARY STRUCTURE IN ELVITEGRAVIR AND DOLUTEGRAVIR COMPLEXES

It was also investigated whether or not transient helix formation occurs in the full length model as it did previously with the CCD [42] (**Fig. 5 and 6**). In the IN-ELV complexes, there is evidence of a transient α-helix conformation in residues 139,146, 147 and 148 in the mutant structures. The Ramachandran plots in Figure 5 show residue 148 with φ and ψ angles corresponding to a β-sheet secondary structure in the WT-ELV complex. However, in the [Q148H, G140S] and [Q148R, G140A] mutants, residue 148 adopts a α-helix secondary structure. (**Fig. 5**). Residue 139 is found in a β-sheet conformation in all complexes except for in [Q148R] where residue 139 is in a right handed helix (**Fig. 5**). Similarly, residue 146 is also in a β-sheet conformation in all complexes except in the [Q148H, G140S] mutant where it exhibits a right handed helix (**Fig. 5**). For residue 147, the WT-ELV and [Q148R, G140A]-ELV complexes have a β-sheet secondary structure. However, in [Q148H], [Q148R], and [N155H, E92Q], residue 147 adopts a left handed α-helix conformation. [Q148H, G140S] adopts a helical conformation as well, but it is right-handed (**Fig. 5**). The mutations at residues 92, 140, 148 and 155 cause the 140s loop (at residues 139, 146, 148 and 147) form a loop that could reduce drug potency; this was observed in prior work with the CCD in complex with RAL [42]. Due to the location of the 140s loop, most likely these residues form a β-strand when in the β-sheet conformation rather than a β-sheet. It is possible that a transient α-helix reduces the flexibility of this region more than a β-strand. Therefore, the reduced flexibility of this region could be attributed to these transient conformational changes.

Evidence of a transient α-helix conformation is also present for the mutant structures at residues 146 and 148 when complexed with DTG. Residue 148 displays a β-sheet conformation

in the WT-DTG complex, whereas in [Q148H, G140S], [Q148R, G140A] and [N155H, E92Q], residue 148 corresponds to the right handed α helix conformation (**Fig.6**). Residue 146 in the WT DTG complex is in a β sheet conformation whereas it is in a right handed helix in the [Q148R] and [N155H, E92Q] complexes (**Fig. 6**).

Figure 4-3: *Secondary structure changes of 140s loop residues in ELV complexes.* The Ramachandran tool in the VMD suite was used to calculate φ and ψ angles of the 140s loop residues in wild type and mutant HIV-1 IN in complex with elvitegravir over the 20000 frame trajectory. Residues displaying the most secondary structural differences are shown.
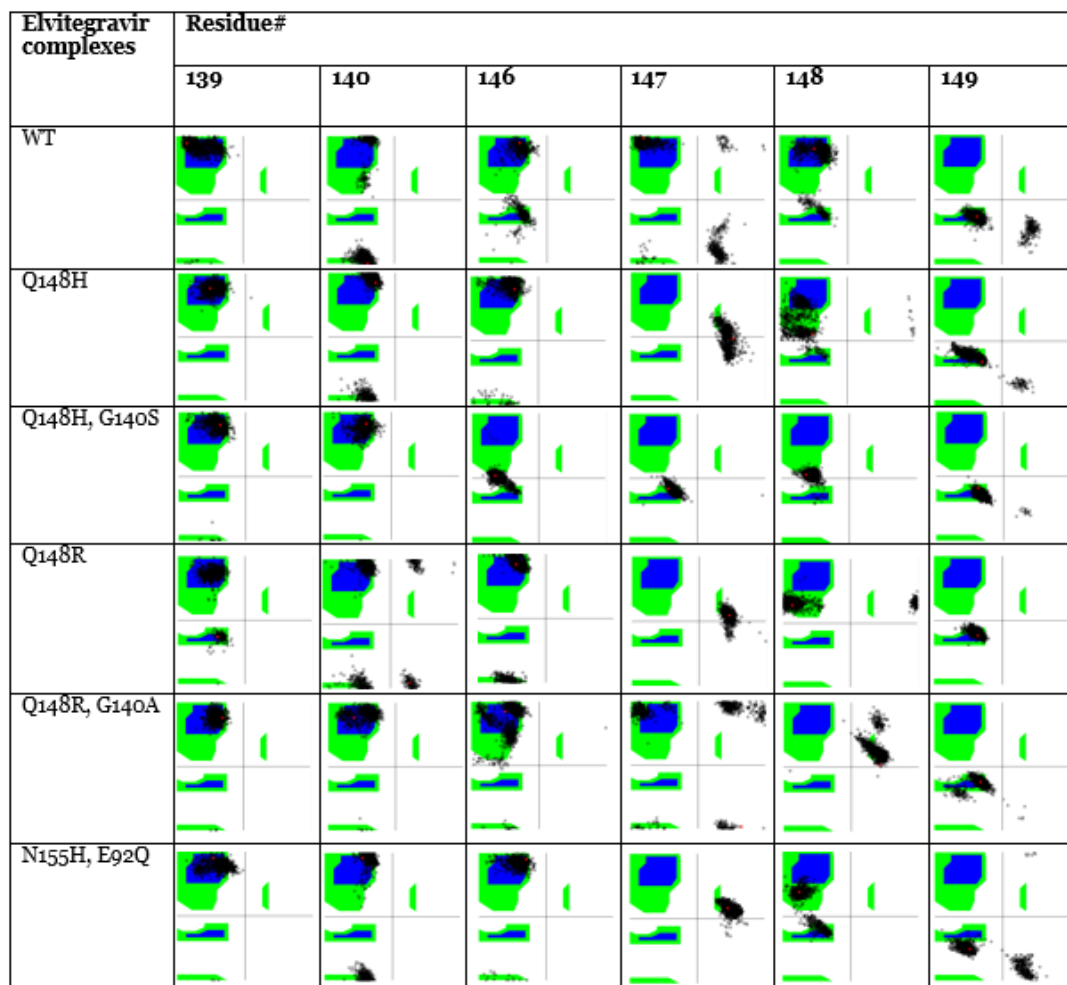
Figure 4-4: *Secondary structure changes of 140s loop residues in DTG complexes.* The Ramachandran tool in the VMD suite was used to calculate φ and ψ angles of the 140s loop residues in wild type and mutant HIV-1 IN in complex with dolutegravir over the 20000 frame trajectory. Residues displaying the most secondary structural differences are shown.
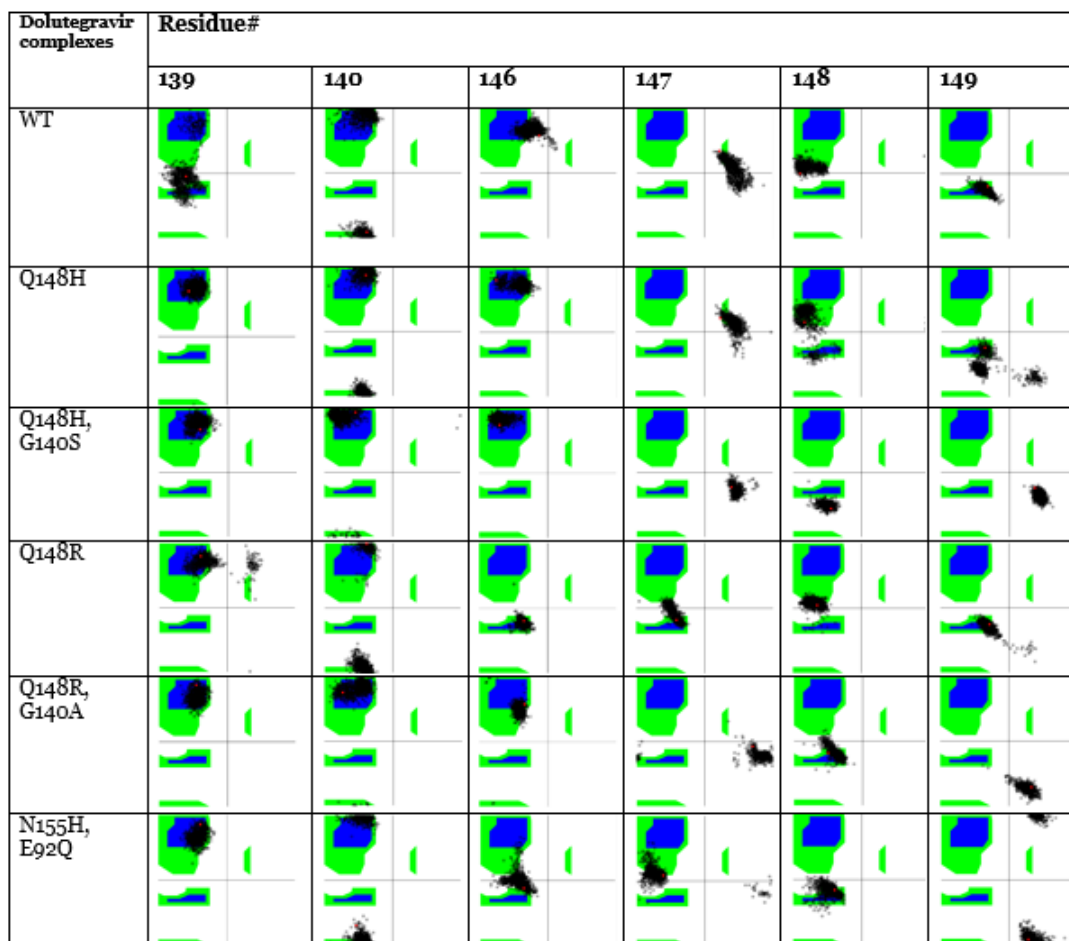
4.2.3 DECREASED FLEXIBILITY OF THE HIV-1 IN MUTANTS RESULT IN ALTERED MOLECULAR RECOGNITION OF HIV-1 INTEGRASE INHIBITORS

Notable changes in molecular recognition of RAL, ELV and DTG by IN occurred in the IN mutant ternary complexes. Interactions between the INSTI and IN, and the INSTI and DNA were quantified every 4 ns of the 40 ns simulation by LigPlot+ and NucPlot and were averaged over these frames[128, 129]. Decreased flexibility of mutant IN alters the binding mode of RAL to the protein and the viral DNA (**Table S1**). All mutant complexes display a decrease in the number of hydrogen bonds compared to the WT-RAL complex, suggesting an altered hydrogen bonding network in the mutant complexes. The [Q148R, G140A] and [Q148H, G140S] mutants contain the fewest hydrogen bonds and van der Waals interactions with RAL as well as decreased RAL-140s loop interactions. This suggests that decreased flexibility through changes in secondary structure of the 140s loop caused by mutations at residues 140 and 148 disrupts RAL stabilizing interactions (**Table S1**).

In the ELV complexes, there were no differences in the hydrogen bond network between IN, viral DNA and ELV except for Q148R hydrogen bonding with ELV in the [Q148R] and [Q148R, G140A] complexes (**Fig. 7**). The positively charged arginine side chain from the Q148R mutation has been noted for its ability to disrupt ELV's chelation mechanism via hydrogen bonding with the ELV carboxyl group [95]. Our LigPlot analysis revealed hydrogen bonds between the ELV carboxyl group and Q148R in the [Q148R] and [Q148R, G140A] mutants. The hydrogen bond between ELV and Q148R is present in all of the frames selected for analysis throughout the entire simulation in these mutants. This is further evidence for the role of Q148R in ELV resistance.

In the IN-DTG complexes, minor differences in the number of hydrogen bonds and van der Waals interactions were observed between DTG, IN, and viral DNA in the mutant complexes compared to the WT complex. As opposed to the RAL complexes, the mutations did not cause any differences in DTG–140s loop interactions nor did they cause changes to the hydrogen bonding network (**Fig. 8**). Non-covalent interactions between viral DNA and DTG, particularly hydrogen bonds and van der Waals interactions, are decreased in the [Q148H, G140S] complex compared to the WT (**Table S2**). [N155H, E92Q] also displays a decrease in van der Waals interactions with viral DNA relative to the WT-DTG complex (**Table S2**).

Table 4-1: Raltegravir interactions with HIV- 1 IN, the 140s loop, and viral DNA.

Mutant studied	Average raltegravir-protein interactions		Average raltegravir 140s loop interactions		Average raltegravir-viral DNA (substrate) interactions	
	H-bonds	van der Waals interactions	H-bonds	van der Waals interactions	H-bonds	vdW interactions
WT	4.4±0.8	33.3±5.7	0.6±0.5	15±4.2	0.0	26.6±5.5
Q148H	4.1±1.4	42.3±5.7	0.4±0.5	15.9±5.3	0.1±0.3	16.8±7.7
Q148H, G140S	3.8±1.0	30.4± 6.5	0.3±0.5	8.7±6.0	0.2±0.4	20.7±11.8
Q148R	3.5±0.8	30.2±9.3	0.2±0.4	10.2±7.0	0.0	11±6.1
Q148R, G140A	3.5±1.4	25±7.0	0.8±0.6	6.5±5.5	0.2±0.4	38.6±10.1
N155H, E92Q	4±0.8	32.4±7.8	0.8±0.4	16.6±6.7	1±0.5	15.6±6.0

Note: LigPlot+ and NucPlot were used to calculate hydrogen (H-bonds) and van der Waals interactions between raltegravir, HIV-1 IN and viral DNA substrate. (Average +/- 1σ). The changes in raltegravir interactions with HIV-1 IN is a result of HIV-1 IN structural alterations.
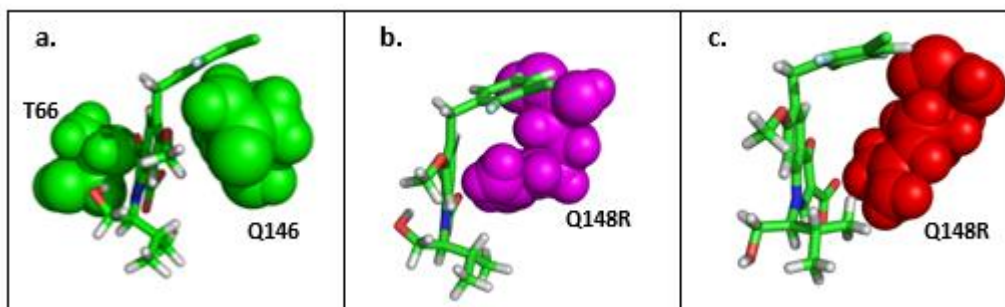
Figure 4-5: *Hydrogen bonding interactions between HIV-1 IN and ELV (A) WT complex (B) Q148R_G140A complex (C) Q148R complex.* Residues involved in hydrogen bond with ELV are shown in sphere representation to demonstrate their van der Waals volume.
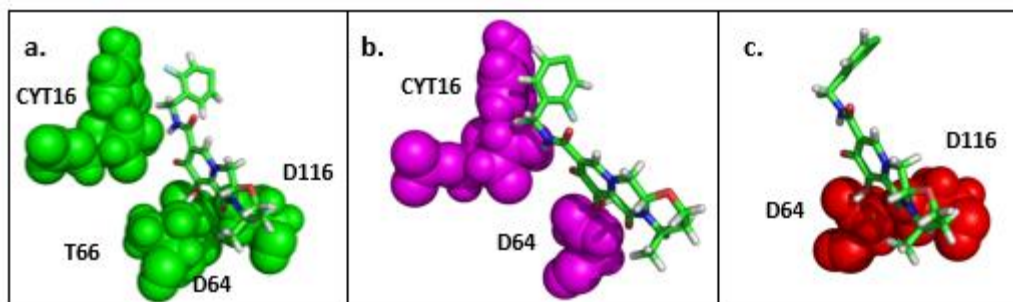
Figure 4-6: *Hydrogen bonding interactions between HIV-1 IN and DTG (A) WT Complex (B) N155H_E92Q Complex (C) Q148H_G140S Complex.* Residues involved in hydrogen bond with RAL are shown in sphere representation to demonstrate their van der Waals volume.

Table 4-2: Dolutegravir interactions with HIV- 1 IN, the 140s loop, and viral DNA

Mutant studied	Average dolutegravir-protein interactions		Average dolutegravir 140s loop interactions		Average dolutegravir- viral DNA (substrate) interactions	
	H-bonds	van der Waals interactions	H-bonds	van der Waals interactions	H-bonds	van der Waals interactions
WT	3.3±1.3	31.8±3.2	0.0	13.4±6.8	1.5±0.7	16.4±4.7
Q148H	2.2±0.9	25.4±3.7	0.0	9.4±2.8	0.9±0.3	22.9±4.9
Q148H, G140S	2.4±1.1	28.8±3.8	0.0	17.6±3.5	0.1±0.3	10.6±3.8
Q148R	2.9±1.4	28.9±8.5	0.8±0.9	14.1±7.2	2.1±0.7	13.1±3.3
Q148R, G140A	2.2±1.0	29.9±5.2	0.0	15±4.1	1.9±0.7	14.1±5.5
N155H, E92Q	2.2±1.0	33.7±5.1	0.0	18.8±5.7	1.5±0.5	13.4±6.2

Note: LigPlot+ and NucPlot were used to calculate hydrogen (H-bonds) and van der Waals interactions between raltegravir, HIV-1 IN and viral DNA substrate. (Average +/- 1σ). The changes in dolutegravir interactions with HIV-1 IN is a result of HIV-1 IN structural alterations.

4.3 DISCUSSION

In this study, the effect of HIV-1 IN mutations [Q148H], [Q148H, G140S], [Q148R], [Q148R, G140A] and [N155H, E92Q] on INSTI-target interactions was investigated. Our results suggest decreased flexibility of IN leads to a change in secondary structure and limited conformational space. The mutations appear to affect IN both locally and globally while also disrupting molecular recognition of RAL and ELV.

4.1 RESISTANCE MUTATIONS AFFECT HIV-1 IN CONFORMATION BOTH LOCALLY AND GLOBALLY.

On a local scale, mutations affect the conformation of the 140s loop and active site, thereby affecting IN and drug interactions. Conformational changes in the [Q148H/R, G140S/A] and [N155H, E92Q] mutants appear to reduce interactions between RAL and the IN 140s loop and viral DNA. Conformational changes in [Q148R] and [Q148R, G140A] caused residue 148 to hydrogen bond with ELV's carboxyl, disrupting its chelation mechanism which is essential for its activity. Also, [Q148H, G140S], [Q148R], [Q148R, G140A] and [N155H, E92Q] all display changes in the secondary structure of the 140s loop when in complex with ELV. These changes may reflect reduced inhibitor–140s loop interactions resulting in lowered RAL and ELV potency. In the DTG complexes, the mutants adopted a α-helix conformation in two residues in the 140s loop relative to IN-ELV complexes (which had 4 residues adopt the α-helix conformation). Also, DTG had similar interactions in the 140s loop when in complex with WT and mutant structures. The mutations affect IN on a global scale as evidenced by the decreased RMSD over all three functional domains compared to the un-complexed WT structure.

4.2 VIRAL SUSCEPTIBILITY DATA (EC$_{50}$) CORRELATES WITH DECREASED FLEXIBILITY AND ALTERED INTERACTION NETWORKS IN SILICO

The results from our *in silico* experiments correlate with reported *in vitro* data presented in **Table 1**. The double mutants ([Q148H, G140S], [Q148R, G140A], and [N155H, E92Q]) display the largest EC$_{50}$ fold change (FC) under RAL and ELV pressure. These mutants display transient secondary structural changes by adopting a α-helical structure in the 140s loop during the 40 ns simulation. Changes in the molecular recognition pattern of RAL are also seen, as indicated by the loss of hydrogen bonds and van der Waals interactions with RAL. Furthermore, IN variants containing the Q148R mutation displayed hydrogen bonds with the key ELV carboxyl group, thereby causing mechanistic disruptions to the ELV chelation mechanism. In addition, interactions between RAL and viral DNA decrease, which are required for ligand specificity and affinity. Decreased flexibility of HIV-1 IN suggests changes in active site conformation may lead to decreased drug binding/potency.
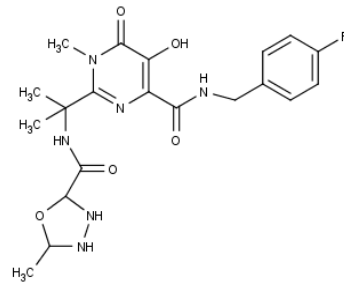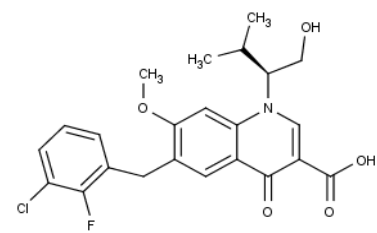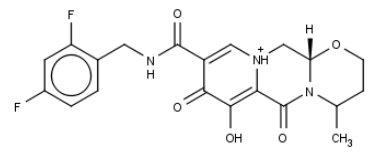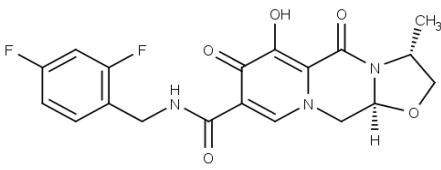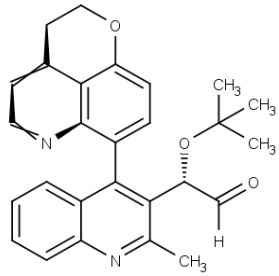
5. CONCLUSION

In conclusion, 40 ns MD simulations revealed mutant forms of IN displayed reduced flexibility, alternative 140s loop secondary structure conformations, and altered molecular recognition patterns compared to the wild-type enzyme. The results presented here with a full length IN model in complex with INSTIs and viral DNA are consistent with our previous reports using the CCD of IN in complex with RAL. Furthermore, the correlation between our results and the reported *in vitro* data shows that this methodology can be a useful drug design and screening tool. For example, *in silico* studies with new inhibitors should reveal similar flexibility patterns between the wild type and a mutant target for optimal inhibitor potency.

CHAPTER 5 : IN SILICO METHODOLOGY TO COMPARE HIV-1 IN STRAND TRANSFER INHIBITORS USING QIKPROP

Qikprop was used to predict the ADME/toxicity (administration, distribution, metabolism, and excretion) parameters of the HIV-1 integrase strand transfer inhibitors raltegravir (RAL), elvitegravir (ELV), dolutegravir (DTG), cabotegravir (CTV) and BI-224436 (BI-22). QikProp is part of the Schrödinger small-molecule drug discovery suite and is used to predict ADME/toxicity properties of preexisting and candidate drugs prior to synthesis and clinical trials for compound modification (Schrödinger, 2013). QikProp also compares molecular properties to preexisting approved drugs. This *in silico* approach saves time, resources and streamlines therapy. Based on the ADME analysis, QikProp calculates stars (descriptor values), which evaluate the organic properties of a drug based on Lipinski's role of five, Jorgenson's rule of three, and ADME factors. Table 6.1 compares the chemical structure and QikProp star values for the first generation INIs RAL and ELV to the second generation INIs DTG, CTV, and BI-22.

Table 5-1: HIV-1 integrase inhibitor Qik Prop ADME stars ratings

HIV- 1 IN generic name	HIV-1 IN inhibitor chemical structure	Qik Prop Stars
Raltegravir		0
Elvitegravir		0
Dolutegravir		0
Cabotegravir		1
BI- 224436		0

RAL, ELV, DTG, CTV, and BI-2 MOL2 files were submitted to QikProp. QikProp generated an output file that listed various ADME/toxicity parameters. The drug's star value reflects how its chemical properties lie within range of the typically approved drug.

All of the inhibitors had a stars score of 0-1 with CTV having the 1 star. CTV has one star because it falls out of range (below) for the human serum albumin binding prediction which is a distribution factor of the drugs pharmacology. However, most of the parameters for CTV are similar to DTG's, indicating that they, theoretically, share an ADME profile. This qualifies CTV as a second generation inhibitor.

REFERENCES

1. Nakashima AK, Fleming PL: HIV/AIDS surveillance in the United States, 1981-2001. *J Acquir Immune Defic Syndr* 2003, 32 Suppl 1:S68–S85.

2. Rubinstein PG, Aboulafia DM, Zloza A: Malignancies in HIV/AIDS: from epidemiology to therapeutic challenges. *AIDS* 2014, 28:453–465.

3. Anderson RM, May RM: Epidemiological parameters of HIV transmission. *Nature* 1988, 333:514–519.

4. Shaw GM, Hunter E: HIV transmission. *Cold Spring Harb Perspect Med* 2012, 2.

5. Prevention C for DC and: Effect of Antiretroviral Therapy on Risk of Sexual Transmission of HIV Infection and Superinfection. 2009.

6. Salomon R: Proteolytic cleavage of the N-terminal region of potyvirus coat protein and its relation to host recovery and vector transmission. *Arch Virol Suppl* 1992, 5:75–76.

7. Sutton MY, Jones RL, Wolitski RJ, Cleveland JC, Dean HD, Fenton KA: A review of the Centers for Disease Control and Prevention's response to the HIV/AIDS crisis among blacks in the United States, 1981-2009. *American Journal of Public Health* 2009.

8. UNAIDS: *GLOBAL REPORT: UNAIDS Report on the Global AIDS Epidemic 2013*. 2013.

9. Watts JM, Dang KK, Gorelick RJ, Leonard CW, Bess JW, Swanstrom R, Burch CL, Weeks KM: Architecture and secondary structure of an entire HIV-1 RNA genome - Supplementary Info. *Nature* 2009, 460:711–6.

10. Al-Hashimi HM: Structural biology: Aerial view of the HIV genome. *Nature* 2009:696–698.

11. Lifson JD, Reyes GR, McGrath MS, Stein BS, Engleman EG: AIDS retrovirus induced cytopathology: giant cell formation and involvement of CD4 antigen. *Science* 1986, 232:1123–1127.

12. Healy EF, Sanders J, King PJ, Robinson Jr. WE: A docking study of L-chicoric acid with HIV-1 integrase. *J Mol Graph Model* 2009, 27:584–589.

13. Briggs JAG, Riches JD, Glass B, Bartonova V, Zanetti G, Kräusslich H-G: Structure and assembly of immature HIV. *Proc Natl Acad Sci U S A* 2009, 106:11090–11095.

14. Zhao G, Perilla JR, Yufenyuy EL, Meng X, Chen B, Ning J, Ahn J, Gronenborn AM, Schulten K, Aiken C, Zhang P: Mature HIV-1 capsid structure by cryo-electron microscopy and all-atom molecular dynamics. *Nature* 2013, 497:643–6.

15. Bukrinsky M: A Hard Way to the Nucleus. *Mol Med* 2004, 10:1–5.

16. Damond F, Lariven S, Roquebert B, Males S, Peytavin G, Morau G, Toledano D, Descamps D, Brun-Vezinet F, Matheron S: Virological and immunological response to HAART regimen containing integrase inhibitors in HIV-2-infected patients. *AIDS* 2008, 22:665–666.

17. Waki K, Sugawara Y: Implications of integrase inhibitors for HIV-infected transplantation recipients: raltegravir and dolutegravir (S/GSK 1349572). *Biosci Trends* 2011, 5:189–191.

18. Hughes A, Barber T, Nelson M: New treatment options for HIV salvage patients: an overview of second generation PIs, NNRTIs, integrase inhibitors and CCR5 antagonists. *J Infect* 2008, 57:1–10.

19. Wang Z, Vince R: Design and synthesis of dual inhibitors of HIV reverse transcriptase and integrase: introducing a diketoacid functionality into delavirdine. *Bioorg Med Chem* 2008, 16:3587–3595.

20. Ruelas DS, Greene WC: An integrated overview of HIV-1 latency. *Cell* 2013, 155:519–529.

21. Shan L, Deng K, Shroff NS, Durand CM, Rabi SA, Yang HC, Zhang H, Margolick JB, Blankson JN, Siliciano RF: Stimulation of HIV-1-specific cytolytic T lymphocytes facilitates elimination of latent viral reservoir after virus reactivation. *Immunity* 2012, 36:491–501.

22. Stellbrink HJ: Raltegravir in the management of HIV-infected patients. *Drug Des Devel Ther* 2009, 2:281–288.

23. Wainberg MA, Mesplede T, Quashie PK: The development of novel HIV integrase inhibitors and the problem of drug resistance. *Curr Opin Virol* 2012, 2:656–662.

24. Yanchunas Jr. J, Langley DR, Tao L, Rose RE, Friborg J, Colonno RJ, Doyle ML: Molecular basis for increased susceptibility of isolates with atazanavir resistance-conferring substitution I50L to other protease inhibitors. *Antimicrob Agents Chemother* 2005, 49:3825–3832.

25. Dolling DI, Dunn DT, Sutherland KA, Pillay D, Mbisa JL, Parry CM, Post FA, Sabin CA, Cane PA, Database UHDR, Study UKCHIVC: Low frequency of genotypic resistance in HIV-1-infected patients failing an atazanavir-containing regimen: a clinical cohort study. *J Antimicrob Chemother* 2013, 68:2339–2343.

26. Clemente JC, Coman RM, Thiaville MM, Janka LK, Jeung JA, Nukoolkarn S, Govindasamy L, Agbandje-McKenna M, McKenna R, Leelamanit W, Goodenow MM, Dunn BM: Analysis of HIV-1 CRF_01 A/E protease inhibitor resistance: structural determinants for maintaining sensitivity and developing resistance to atazanavir. *Biochemistry* 2006, 45:5468–5477.

27. HIV-1 Reverse Transcriptase [http://maptest.rutgers.edu/drupal/?q=node/198]

28. He HQ, Ma XH, Liu B, Chen WZ, Wang CX, Cheng SH: A novel high-throughput format assay for HIV-1 integrase strand transfer reaction using magnetic beads. *Acta Pharmacol Sin* 2008, 29:397–404.

29. Liu Z, Wang Y, Yedidi RS, Dewdney TG, Reiter SJ, Brunzelle JS, Kovari IA, Kovari LC: Conserved hydrogen bonds and water molecules in MDR HIV-1 protease substrate complexes. *Biochem Biophys Res Commun* 2013, 430:1022–1027.

30. Zheng R, Jenkins TM, Craigie R: Zinc folds the N-terminal domain of HIV-1 integrase,

promotes multimerization, and enhances catalytic activity. *Proc Natl Acad Sci U S A* 1996, 93:13659–13664.

31. Delelis O, Carayon K, Saib A, Deprez E, Mouscadet JF: Integrase and integration: biochemical activities of HIV-1 integrase. *Retrovirology* 2008, 5:114.

32. Eijkelenboom AP, van den Ent FM, Vos A, Doreleijers JF, Hard K, Tullius TD, Plasterk RH, Kaptein R, Boelens R: The solution structure of the amino-terminal HHCC domain of HIV-2 integrase: a three-helix bundle stabilized by zinc. *Curr Biol* 1997, 7:739–746.

33. Bushman FD, Engelman A, Palmer I, Wingfield P, Craigie R: Domains of the integrase protein of human immunodeficiency virus type 1 responsible for polynucleotidyl transfer and zinc binding. *Proc Natl Acad Sci U S A* 1993, 90:3428–3432.

34. Schauer M, Billich A: The N-terminal region of HIV-1 integrase is required for integration activity, but not for DNA-binding. *Biochem Biophys Res Commun* 1992, 185:874–880.

35. Burke CJ, Sanyal G, Bruner MW, Ryan JA, LaFemina RL, Robbins HL, Zeft AS, Middaugh CR, Cordingley MG: Structural implications of spectroscopic characterization of a putative zinc finger peptide from HIV-1 integrase. *J Biol Chem* 1992, 267:9639–9644.

36. Lins RD, Adesokan A, Soares TA, Briggs JM: Investigations on human immunodeficiency virus type 1 integrase/DNA binding interactions via molecular dynamics and electrostatics calculations. *Pharmacol Ther* 2000, 85:123–131.

37. Pommier Y, Johnson AA, Marchand C: Integrase inhibitors to treat HIV/AIDS. *Nat Rev Drug Discov* 2005, 4:236–248.

38. Maignan S, Guilloteau JP, Zhou-Liu Q, Clement-Mella C, Mikol V: Crystal structures of the catalytic domain of HIV-1 integrase free and complexed with its metal cofactor: high level of similarity of the active site with other viral integrases. *J Mol Biol* 1998, 282:359–368.

39. Lins RD, Briggs JM, Straatsma TP, Carlson HA, Greenwald J, Choe S, McCammon JA: Molecular dynamics studies on the HIV-1 integrase catalytic domain. *Biophys J* 1999, 76:2999–3011.

40. Greenwald J, Le V, Butler SL, Bushman FD, Choe S: The mobility of an HIV-1 integrase active site loop is correlated with catalytic activity. *Biochemistry* 1999, 38:8892–8898.

41. Hare S, Smith SJ, Metifiot M, Jaxa-Chamiec A, Pommier Y, Hughes SH, Cherepanov P: Structural and functional analyses of the second-generation integrase strand transfer inhibitor dolutegravir (S/GSK1349572). *Mol Pharmacol* 2011, 80:565–572.

42. Dewdney TG, Wang Y, Kovari IA, Reiter SJ, Kovari LC: Reduced HIV-1 integrase flexibility as a mechanism for raltegravir resistance. *J Struct Biol* 2013, 184:245–250.

43. DeAnda F, Hightower KE, Nolte RT, Hattori K, Yoshinaga T, Kawasuji T, Underwood MR: Dolutegravir interactions with HIV-1 integrase-DNA: structural rationale for drug resistance and dissociation kinetics. *PLoS One* 2013, 8:e77448.

44. Chen JC, Krucinski J, Miercke LJ, Finer-Moore JS, Tang AH, Leavitt AD, Stroud RM: Crystal structure of the HIV-1 integrase catalytic core and C-terminal domains: a model for viral DNA binding. *Proc Natl Acad Sci U S A* 2000, 97:8233–8238.

45. Singh SB, Felock P, Hazuda DJ: Chemical and enzymatic modifications of integric acid and HIV-1 integrase inhibitory activity. *Bioorg Med Chem Lett* 2000, 10:235–238.

46. Brin E, Yi J, Skalka AM, Leis J: Modeling the late steps in HIV-1 retroviral integrase-catalyzed DNA integration. *J Biol Chem* 2000, 275:39287–39295.

47. Bushman FD, Fujiwara T, Craigie R: Retroviral DNA integration directed by HIV integration protein in vitro. *Science (80-)* 1990, 249:1555–1558.

48. Drelich M, Wilhelm R, Mous J: Identification of amino acid residues critical for endonuclease

and integration activities of HIV-1 IN protein in vitro. *Virology* 1992, 188:459–468.

49. Kang SY, Ahn DG, Lee C, Lee YS, Shin CG: Functional nucleotides of U5 LTR determining substrate specificity of prototype foamy virus integrase. *J Microbiol Biotechnol* 2008, 18:1044–1049.

50. Li M, Craigie R: Processing of viral DNA ends channels the HIV-1 integration reaction to concerted integration. *J Biol Chem* 2005, 280:29334–29339.

51. Farnet CM, Wang B, Lipford JR, Bushman FD: Differential inhibition of HIV-1 preintegration complexes and purified integrase protein by small molecules. *Proc Natl Acad Sci U S A* 1996, 93:9742–9747.

52. Engelman A, Cherepanov P: The lentiviral integrase binding protein LEDGF/p75 and HIV-1 replication. *PLoS Pathog* 2008, 4:e1000046.

53. Devroe E, Engelman A, Silver PA: Intracellular transport of human immunodeficiency virus type 1 integrase. *J Cell Sci* 2003, 116(Pt 21):4401–4408.

54. Vink C, Lutzke RA, Plasterk RH: Formation of a stable complex between the human immunodeficiency virus integrase protein and viral DNA. *Nucleic Acids Res* 1994, 22:4103–4110.

55. Vaisocherova H, Snasel J, Springer T, Sipova H, Rosenberg I, Stepanek J, Homola J: Surface plasmon resonance study on HIV-1 integrase strand transfer activity. *Anal Bioanal Chem* 2009, 393:1165–1172.

56. Hare S, Gupta SS, Valkov E, Engelman A, Cherepanov P: Retroviral intasome assembly and inhibition of DNA strand transfer. *Nature* 2010, 464:232–236.

57. Lee-Huang S, Huang PL, Huang PL, Bourinbaiar AS, Chen HC, Kung HF: Inhibition of the integrase of human immunodeficiency virus (HIV) type 1 by anti-HIV plant proteins MAP30 and GAP31. *Proc Natl Acad Sci U S A* 1995, 92:8818–8822.

58. Faust EA, Garg A, Small L, Acel A, Wald R, Udashkin B: Enzymatic Capability of HIS-Tagged HIV-1 Integrase Using Oligonucleotide Disintegration Substrates. *J Biomed Sci* 1996, 3:254–265.

59. Chow SA, Vincent KA, Ellison V, Brown PO: Reversal of integration and DNA splicing mediated by integrase of human immunodeficiency virus. *Science (80-)* 1992, 255:723–726.

60. Raghavendra NK, Shkriabai N, Graham RL, Hess S, Kvaratskhelia M, Wu L: Identification of host proteins associated with HIV-1 preintegration complexes isolated from infected CD4+ cells. *Retrovirology* 2010, 7:66.

61. Wei SQ, Mizuuchi K, Craigie R: A large nucleoprotein assembly at the ends of the viral DNA mediates retroviral DNA integration. *EMBO J* 1997, 16:7511–7520.

62. Dolan J, Chen A, Weber IT, Harrison RW, Leis J: Defining the DNA substrate binding sites on HIV-1 integrase. *J Mol Biol* 2009, 385:568–579.

63. Fenwick C, Amad M, Bailey MD, Bethell R, Bos M, Bonneau P, Cordingley M, Coulombe R, Duan J, Edwards P, Fader LD, Faucher AM, Garneau M, Jakalian A, Kawai S, Lamorte L, LaPlante S, Luo L, Mason S, Poupart MA, Rioux N, Schroeder P, Simoneau B, Tremblay S, Tsantrizos Y, Witvrouw M, Yoakim C: Preclinical Profile of BI 224436, a Novel HIV-1 Non-Catalytic-Site Integrase Inhibitor. *Antimicrob Agents Chemother* 2014, 58:3233–3244.

64. Wielens J, Crosby IT, Chalmers DK: A three-dimensional model of the human immunodeficiency virus type 1 integration complex. *J Comput Aided Mol Des* 2005, 19:301–317.

65. Agapkina J, Smolov M, Barbe S, Zubin E, Zatsepin T, Deprez E, Le Bret M, Mouscadet JF, Gottikh M: Probing of HIV-1 integrase/DNA interactions using novel analogs of viral DNA. *J Biol Chem* 2006, 281:11530–11540.

66. Lu R, Limon A, Ghory HZ, Engelman A: Genetic analyses of DNA-binding mutants in the

catalytic core domain of human immunodeficiency virus type 1 integrase. *J Virol* 2005, 79:2493–2505.

67. Reil H, Bukovsky AA, Gelderblom HR, Göttlinger H: Efficient HIV-1 replication can occur in the absence of the viral matrix protein. *EMBO J* 1998, 17:2699–2708.

68. Chen H, Engelman A: The barrier-to-autointegration protein is a host factor for HIV type 1 integration. *Proc Natl Acad Sci U S A* 1998, 95:15270–15274.

69. Hamamoto S, Nishitsuji H, Amagasa T, Kannagi M, Masuda T: Identification of a novel human immunodeficiency virus type 1 integrase interactor, Gemin2, that facilitates efficient viral cDNA synthesis in vivo. *J Virol* 2006, 80:5670–5677.

70. Cereseto A, Manganaro L, Gutierrez MI, Terreni M, Fittipaldi A, Lusic M, Marcello A, Giacca M: Acetylation of HIV-1 integrase by p300 regulates viral integration. *EMBO J* 2005, 24:3070–3081.

71. Farnet CM, Bushman FD: HIV-1 cDNA integration: Requirement of HMG I(Y) protein for function of preintegration complexes in vitro. *Cell* 1997, 88:483–492.

72. Parissi V, Calmels C, De Soultrait VR, Caumont A, Fournier M, Chaignepain S, Litvak S: Functional interactions of human immunodeficiency virus type 1 integrase with human and yeast HSP60. *J Virol* 2001, 75:11344–11353.

73. Violot S, Hong SS, Rakotobe D, Petit C: The human polycomb group EED protein interacts with the integrase of human immunodeficiency virus type 1. *J ...* 2003.

74. Ao Z, Huang G, Yao H, Xu Z, Labine M, Cochrane AW, Yao X: Interaction of human immunodeficiency virus type 1 integrase with cellular nuclear import receptor importin 7 and its impact on viral replication. *J Biol Chem* 2007, 282:13456–13467.

75. Kalpana G V, Marmon S, Wang W, Crabtree GR, Goff SP: Binding and stimulation of HIV-1

integrase by a human homolog of yeast transcription factor SNF5. *Science* 1994, 266:2002–2006.

76. Poeschla EM: Integrase, LEDGF/p75 and HIV replication. *Cell Mol Life Sci* 2008, 65:1403–1424.

77. Cherepanov P, Maertens G, Proost P, Devreese B, Van Beeumen J, Engelborghs Y, De Clercq E, Debyser Z: HIV-1 integrase forms stable tetramers and associates with LEDGF/p75 protein in human cells. *J Biol Chem* 2003, 278:372–381.

78. Willetts KE, Rey F, Agostini I, Navarro JM, Baudat Y, Vigne R, Sire J: DNA repair enzyme uracil DNA glycosylase is specifically incorporated into human immunodeficiency virus type 1 viral particles through a Vpr-independent mechanism. *J Virol* 1999, 73:1682–1688.

79. Christ F, Debyser Z: The LEDGF/p75 integrase interaction, a novel target for anti-HIV therapy. *Virology* 2013, 435:102–109.

80. Espeseth AS, Felock P, Wolfe A, Witmer M, Grobler J, Anthony N, Egbertson M, Melamed JY, Young S, Hamill T, Cole JL, Hazuda DJ: HIV-1 integrase inhibitors that compete with the target DNA substrate define a unique strand transfer conformation for integrase. *Proc Natl Acad Sci U S A* 2000, 97:11244–11249.

81. Marchand C, Zhang X, Pais GC, Cowansage K, Neamati N, Burke Jr. TR, Pommier Y: Structural determinants for HIV-1 integrase inhibition by beta-diketo acids. *J Biol Chem* 2002, 277:12596–12603.

82. Grobler JA, Stillmock K, Hu B, Witmer M, Felock P, Espeseth AS, Wolfe A, Egbertson M, Bourgeois M, Melamed J, Wai JS, Young S, Vacca J, Hazuda DJ: Diketo acid inhibitor mechanism and HIV-1 integrase: implications for metal binding in the active site of phosphotransferase enzymes. *Proc Natl Acad Sci U S A* 2002, 99:6661–6666.

83. Hazuda DJ, Felock P, Witmer M, Wolfe A, Stillmock K, Grobler JA, Espeseth A, Gabryelski

L, Schleif W, Blau C, Miller MD: Inhibitors of strand transfer that prevent integration and inhibit HIV-1 replication in cells. *Science (80-)* 2000, 287:646–650.

84. Buzon MJ, Marfil S, Puertas MC, Garcia E, Clotet B, Ruiz L, Blanco J, Martinez-Picado J, Cabrera C: Raltegravir susceptibility and fitness progression of HIV type-1 integrase in patients on long-term antiretroviral therapy. *Antivir Ther* 2008, 13:881–893.

85. DeJesus E, Rockstroh JK, Henry K, Molina JM, Gathe J, Ramanathan S, Wei X, Yale K, Szwarcberg J, White K, Cheng AK, Kearney BP, Team GSS: Co-formulated elvitegravir, cobicistat, emtricitabine, and tenofovir disoproxil fumarate versus ritonavir-boosted atazanavir plus co-formulated emtricitabine and tenofovir disoproxil fumarate for initial treatment of HIV-1 infection: a randomised, double-. *Lancet* 2012, 379:2429–2438.

86. Blanco Arevalo JL, Whitlock GG: Dolutegravir: an exciting new kid on the block. *Expert Opin Pharmacother* 2014, 15:573–582.

87. INSENTRESS [http://www.rxlist.com/isentress-drug/clinical-pharmacology.htm]

88. Saag MS: New and investigational antiretroviral drugs for HIV infection: mechanisms of action and early research findings. *Top Antivir Med* 2012, 20:162–167.

89. Mouscadet J-F: RALTEGRAVIR: MOLECULAR BASIS OF ITS MECHANISM OF ACTION. *Eur J Med Res* 2009, 14:5– 16.

90. Hare S, Vos AM, Clayton RF, Thuring JW, Cummings MD, Cherepanov P: Molecular mechanisms of retroviral integrase inhibition and the evolution of viral resistance. *Proc Natl Acad Sci U S A* 2010, 107:20057–20062.

91. Pandey KK: Critical appraisal of elvitegravir in the treatment of HIV-1/AIDS. *HIV AIDS* 2014, 6:81–90.

92. US guidelines include Stribild (Quad) as alternative rather than preferred option for treatment

naive adults [http://i-base.info/htb/20290]

93. Andersen K: Gilead Sciences Carving Out a Wider Moat . 2012.

94. Shimura K, Kodama EN: Elvitegravir: a new HIV integrase inhibitor. *Antivir Chem Chemother* 2009, 20:79–85.

95. DeAnda F, Hightower KE, Nolte RT, Hattori K, Yoshinaga T, Kawasuji T, Underwood MR: Dolutegravir Interactions with HIV-1 Integrase-DNA: Structural Rationale for Drug Resistance and Dissociation Kinetics. *PLoS One* 2013, 8.

96. Castagna A, Maggiolo F, Penco G, Wright D, Mills A, Grossberg R, Molina JM, Chas J, Durant J, Moreno S, Doroana M, Ait-Khaled M, Huang J, Min S, Song I, Vavro C, Nichols G, Yeo JM, for the V-SG: Dolutegravir in Antiretroviral-Experienced Patients With Raltegravir- and/or Elvitegravir-Resistant HIV-1: 24-Week Results of the Phase III VIKING-3 Study. *J Infect Dis* 2014.

97. Dolutegravir [http://www.allfordrugs.com/?s=dolutegravir&searchsubmit=]

98. Castellino S, Moss L, Wagner D, Borland J, Song I, Chen S, Lou Y, Min SS, Goljer I, Culp A, Piscitelli SC, Savina PM: Metabolism, excretion, and mass balance of the HIV-1 integrase inhibitor dolutegravir in humans. *Antimicrob Agents Chemother* 2013, 57:3536–3546.

99. Raffi F, Rachlis A, Stellbrink HJ, Hardy WD, Torti C, Orkin C, Bloch M, Podzamczer D, Pokrovsky V, Pulido F, Almond S, Margolis D, Brennan C, Min S, Group S-S: Once-daily dolutegravir versus raltegravir in antiretroviral-naive adults with HIV-1 infection: 48 week results from the randomised, double-blind, non-inferiority SPRING-2 study. *Lancet* 2013, 381:735–743.

100. Cada DJ, Levien TL, Baker DE: Dolutegravir. *Hosp Pharm* 2014, 49:184–195.

101. Spreen W, Min S, Ford SL, Chen S, Lou Y, Bomar M, St Clair M, Piscitelli S, Fujiwara T: Pharmacokinetics, safety, and monotherapy antiviral activity of GSK1265744, an HIV integrase

strand transfer inhibitor. *HIV Clin Trials* 2013, 14:192–203.

102. Johns BA, Kawasuji T, Weatherhead JG, Taishi T, Temelkoff DP, Yoshida H, Akiyama T, Taoda Y, Murai H, Kiyama R, Fuji M, Tanimoto N, Jeffrey J, Foster SA, Yoshinaga T, Seki T, Kobayashi M, Sato A, Johnson MN, Garvey EP, Fujiwara T: Carbamoyl pyridone HIV-1 integrase inhibitors 3. A diastereomeric approach to chiral nonracemic tricyclic ring systems and the discovery of dolutegravir (S/GSK1349572) and (S/GSK1265744). *J Med Chem* 2013, 56:5901–5916.

103. Highleyman L: ICAAC 2013: New Integrase Inhibitor GSK1265744 Safe and Well-tolerated in 8 Studies . .

104. Highleyman L: ICAAC 2011: New Integrase Inhibitor BI 224436 Active against Raltegravir-Resistant HIV . .

105. Karmon SL, Markowitz M: Next-generation integrase inhibitors : where to after raltegravir? *Drugs* 2013, 73:213–228.

106. Fader LD, Malenfant E, Parisien M, Carson R, Bilodeau F, Landry S, Pesant M, Brochu C, Morin S, Chabot C, Halmos T, Bousquet Y, Bailey MD, Kawai SH, Coulombe R, LaPlante S, Jakalian A, Bhardwaj PK, Wernic D, Schroeder P, Amad M, Edwards P, Garneau M, Duan J, Cordingley M, Bethell R, Mason SW, Bos M, Bonneau P, Poupart MA, et al.: Discovery of BI 224436, a Noncatalytic Site Integrase Inhibitor (NCINI) of HIV-1. *ACS Med Chem Lett* 2014, 5:422–427.

107. Liedtke MD, Tomlin CR, Lockhart SM, Miller MM, Rathbun RC: Long-term efficacy and safety of raltegravir in the management of HIV infection. *Infect Drug Resist* 2014, 7:73–84.

108. Varghese V, Liu TF, Rhee SY, Libiran P, Trevino C, Fessel WJ, Shafer RW: HIV-1 integrase sequence variability in antiretroviral naive patients and in triple-class experienced patients

subsequently treated with raltegravir. *AIDS Res Hum Retroviruses* 2010, 26:1323–1326.

109. da Silva D, Van Wesenbeeck L, Breilh D, Reigadas S, Anies G, Van Baelen K, Morlat P, Neau D, Dupon M, Wittkop L, Fleury H, Masquelier B: HIV-1 resistance patterns to integrase inhibitors in antiretroviral-experienced patients with virological failure on raltegravir-containing regimens. *J Antimicrob Chemother* 2010, 65:1262–1269.

110. Cooper DA, Steigbigel RT, Gatell JM, Rockstroh JK, Katlama C, Yeni P, Lazzarin A, Clotet B, Kumar PN, Eron JE, Schechter M, Markowitz M, Loutfy MR, Lennox JL, Zhao J, Chen J, Ryan DM, Rhodes RR, Killar JA, Gilde LR, Strohmaier KM, Meibohm AR, Miller MD, Hazuda DJ, Nessly ML, DiNubile MJ, Isaacs RD, Teppler H, Nguyen BY, Teams BS: Subgroup and resistance analyses of raltegravir for resistant HIV-1 infection. *N Engl J Med* 2008, 359:355–365.

111. Fransen S, Gupta S, Danovich R, Hazuda D, Miller M, Witmer M, Petropoulos CJ, Huang W: Loss of raltegravir susceptibility by human immunodeficiency virus type 1 is conferred via multiple nonoverlapping genetic pathways. *J Virol* 2009, 83:11440–11446.

112. Goethals O, Vos A, Van Ginderen M, Geluykens P, Smits V, Schols D, Hertogs K, Clayton R: Primary mutations selected in vitro with raltegravir confer large fold changes in susceptibility to first-generation integrase inhibitors, but minor fold changes to inhibitors with second-generation resistance profiles. *Virology* 2010, 402:338–346.

113. Kobayashi M, Yoshinaga T, Seki T, Wakasa-Morimoto C, Brown KW, Ferris R, Foster SA, Hazen RJ, Miki S, Suyama-Kagitani A, Kawauchi-Miki S, Taishi T, Kawasuji T, Johns BA, Underwood MR, Garvey EP, Sato A, Fujiwara T: In vitro antiretroviral properties of S/GSK1349572, a next-generation HIV integrase inhibitor. *Antimicrob Agents Chemother* 2011, 55:813–821.

114. Malet I, Delelis O, Valantin MA, Montes B, Soulie C, Wirden M, Tchertanov L, Peytavin G,

Reynes J, Mouscadet JF, Katlama C, Calvez V, Marcelin AG: Mutations associated with failure of raltegravir treatment affect integrase sensitivity to the inhibitor in vitro. *Antimicrob Agents Chemother* 2008, 52:1351–1358.

115. Integrase Inhibitor (INI) Resistance Notes. 2014.

116. Blanco JL, Varghese V, Rhee SY, Gatell JM, Shafer RW: HIV-1 integrase inhibitor resistance and its clinical implications. *J Infect Dis* 2011, 203:1204–1214.

117. Wensing AM, Calvez V, Günthard HF, Johnson V a, Paredes R, Pillay D, Shafer RW, Richman DD: 2014 update of the drug resistance mutations in HIV-1. *Top Antivir Med* 2014, 22:642–50.

118. Abram ME, Hluhanich RM, Goodman DD, Andreatta KN, Margot NA, Ye LD, Niedziela-Majka A, Barnes TL, Novikov N, Chen XW, Svarovskaia ES, McColl DJ, White KL, Miller MD: Impact of Primary Elvitegravir Resistance-Associated Mutations in HIV-1 Integrase on Drug Susceptibility and Viral Replication Fitness. *Antimicrob Agents Chemother* 2013, 57:2654–2663.

119. Goethals O, Clayton R, Van Ginderen M, Vereycken I, Wagemans E, Geluykens P, Dockx K, Strijbos R, Smits V, Vos A, Meersseman G, Jochmans D, Vermeire K, Schols D, Hallenberger S, Hertogs K: Resistance mutations in human immunodeficiency virus type 1 integrase selected with elvitegravir confer reduced susceptibility to a wide range of integrase inhibitors. *J Virol* 2008, 82:10366–10374.

120. Winters MA, Lloyd RM, Shafer RW, Kozal MJ, Miller MD, Holodniy M: Development of elvitegravir resistance and linkage of integrase inhibitor mutations with protease and reverse transcriptase resistance mutations. *PLoS One* 2012, 7.

121. Humphrey W, Dalke A, Schulten K: VMD: visual molecular dynamics. *J Mol Graph* 1996, 14:27–28,33–38.

122. Vanommeslaeghe K, Hatcher E, Acharya C, Kundu S, Zhong S, Shim J, Darian E, Guvench O, Lopes P, Vorobyov I, Mackerell AD: CHARMM general force field: A force field for drug-like molecules compatible with the CHARMM all-atom additive biological force fields. *J Comput Chem* 2010, 31:671–690.

123. Phillips JC, Braun R, Wang W, Gumbart J, Tajkhorshid E, Villa E, Chipot C, Skeel RD, Kale L, Schulten K: Scalable molecular dynamics with NAMD. *J Comput Chem* 2005, 26:1781–1802.

124. Sotomayor M, Schulten K: Molecular dynamics study of gating in the mechanosensitive channel of small conductance MscS. *Biophys J* 2004, 87:3050–3065.

125. Hsu CK, Park S: Computational and mutagenesis studies of the streptavidin native dimer interface. *J Mol Graph Model* 2010, 29:295–308.

126. Schwede T, Kopp J, Guex N, Peitsch MC: SWISS-MODEL: An automated protein homology-modeling server. *Nucleic Acids Res* 2003, 31:3381–3385.

127. Guex N, Peitsch MC: SWISS-MODEL and the Swiss-PdbViewer: An environment for comparative protein modeling. *Electrophoresis* 1997, 18:2714–2723.

128. Laskowski RA, Swindells MB: LigPlot+: Multiple ligand-protein interaction diagrams for drug discovery. *J Chem Inf Model* 2011, 51:2778–2786.

129. Luscombe NM, Laskowski RA, Thornton JM: NUCPLOT: A program to generate schematic diagrams of protein-nucleic acid interactions. *Nucleic Acids Res* 1997, 25:4940–4945.

130. Metifiot M, Maddali K, Naumova A, Zhang X, Marchand C, Pommier Y: Biochemical and pharmacological analyses of HIV-1 integrase flexible loop mutants resistant to raltegravir. *Biochemistry* 2010, 49:3715–3722.

131. Johnson AA, Santos W, Pais GC, Marchand C, Amin R, Burke Jr. TR, Verdine G, Pommier Y: Integration requires a specific interaction of the donor DNA terminal 5'-cytosine with

glutamine 148 of the HIV-1 integrase flexible loop. *J Biol Chem* 2006, 281:461–467.

132. Bacchi A, Carcelli M, Compari C, Fisicaro E, Pala N, Rispoli G, Rogolino D, Sanchez TW, Sechi M, Sinisi V, Neamati N: Investigating the role of metal chelation in HIV-1 integrase strand transfer inhibitors. *J Med Chem* 2011, 54:8407–8420.

133. Perryman AL, Forli S, Morris GM, Burt C, Cheng Y, Palmer MJ, Whitby K, McCammon JA, Phillips C, Olson AJ: A dynamic model of HIV integrase inhibition and drug resistance. *J Mol Biol* 2010, 397:600–615.

134. Underwood MR, Johns BA, Sato A, Martin JN, Deeks SG, Fujiwara T: The activity of the integrase inhibitor dolutegravir against HIV-1 variants isolated from raltegravir-treated adults. *J Acquir Immune Defic Syndr* 2012, 61:297–301.

135. Hu Z, Kuritzkes DR: Effect of raltegravir resistance mutations in HIV-1 integrase on viral fitness. *J Acquir Immune Defic Syndr* 2010, 55:148–155.

136. Canducci F, Ceresola ER, Boeri E, Spagnuolo V, Cossarini F, Castagna A, Lazzarin A, Clementi M: Cross-resistance profile of the novel integrase inhibitor Dolutegravir (S/GSK1349572) using clonal viral variants selected in patients failing raltegravir. *J Infect Dis* 2011, 204:1811–1815.

137. Ceccherini-Silberstein F, Van Baelen K, Armenia D, Trignetti M, Rondelez E, Fabeni L, Scopelliti F, Pollicita M, Van Wesenbeeck L, Van Eygen V, Dori L, Sarmati L, Aquaro S, Palamara G, Andreoni M, Stuyver LJ, Perno CF: Secondary integrase resistance mutations found in HIV-1 minority quasispecies in integrase therapy-naive patients have little or no effect on susceptibility to integrase inhibitors. *Antimicrob Agents Chemother* 2010, 54:3938–3948.

138. Hightower KE, Wang R, Deanda F, Johns BA, Weaver K, Shen Y, Tomberlin GH, Carter 3rd HL, Broderick T, Sigethy S, Seki T, Kobayashi M, Underwood MR: Dolutegravir

(S/GSK1349572) exhibits significantly slower dissociation than raltegravir and elvitegravir from wild-type and integrase inhibitor-resistant HIV-1 integrase-DNA complexes. *Antimicrob Agents Chemother* 2011, 55:4552–4559.

139. Malet I, Delelis O, Soulie C, Wirden M, Tchertanov L, Mottaz P, Peytavin G, Katlama C, Mouscadet JF, Calvez V, Marcelin AG: Quasispecies variant dynamics during emergence of resistance to raltegravir in HIV-1-infected patients. *J Antimicrob Chemother* 2009, 63:795–804.

140. Witmer M, Danovich R: Selection and analysis of HIV-1 integrase strand transfer inhibitor resistant mutant viruses. *Methods* 2009, 47:277–282.

141. Piana S, Carloni P, Rothlisberger U: Drug resistance in HIV-1 protease: Flexibility-assisted mechanism of compensatory mutations. *Protein Sci* 2002, 11:2393–2402.

142. Mittal S: Role of Protein Flexibility in Function, Resistance Pathways and Substrate Recognition Specificity in HIV-1 Protease: A Dissertation. University of Massachusetts; 2011.

143. Vavro C, Hasan S, Madsen H, Horton J, DeAnda F, Martin-Carpenter L, Sato A, Cuffe R, Chen S, Underwood M, Nichols G: Prevalent polymorphisms in wild-type HIV-1 integrase are unlikely to engender drug resistance to dolutegravir (S/GSK1349572). *Antimicrob Agents Chemother* 2013, 57:1379–1384.

144. Rhee SY, Taylor J, Fessel WJ, Kaufman D, Towner W, Troia P, Ruane P, Hellinger J, Shirvani V, Zolopa A, Shafer RW: HIV-1 protease mutations and protease inhibitor cross-resistance. *Antimicrob Agents Chemother* 2010, 54:4253–4261.

145. Rhee S-Y, Gonzales MJ, Kantor R, Betts BJ, Ravela J, Shafer RW: Human immunodeficiency virus reverse transcriptase and protease sequence database. *Nucleic Acids Res* 2003, 31:298–303.

146. Schrodinger: QikProp. 2013.

ABSTRACT

HIV INTEGRASE MECHANISMS OF RESISTANCE TO RALTEGRAVIR, ELVITEGRAVIR, AND DOLUTEGRAVIR

by

KYLA ROSS

December 2015

Advisor: Dr. Ladislau Kovari

Major: Biochemistry and Molecular Biology

Degree: Master of Science

HIV-1 integrase (HIV-1 IN or IN) is a multimeric enzyme that integrates the HIV-1 genome into the chromosomes of infected CD4+ T-cells. Currently there are three FDA approved HIV-1 IN strand transfer inhibitors (INSTIs) used in clinical practice: raltegravir (RAL), elvitegravir (ELV), and dolutegravir (DTG). The [Q148H], [Q148H, G140S], [Q148R], [Q148R, G140A] and [N155H, E92Q] mutations decrease IN susceptibility to RAL and ELV and may result in therapeutic failure. As an indicator of protein flexibility, the root mean square deviation (RMSD) of each HIV-1 IN residue in the last 5 ns of a 40 ns molecular dynamics simulation was calculated for HIV-1 IN catalytic core domain as an apoprotein and in complex with RAL, ELV, and DTG to study how the mutations affect HIV-1 IN flexibility. In addition, we studied the relationship between HIV-1 IN flexibility and resistance. We found that the mutants reduced overall HIV-1 IN flexibility relative to the WT IN apoprotein. We also observed that the catalytic 140s loop in the HIV-1 IN-INSTI complexes were more flexible in mutants that displayed higher reported EC_{50} FC (fold change) values. To further investigate the mutations effect on the more complexed full length HIV-1 IN structure, we used molecular dynamics simulations to study the

impact of the mutants on binary (IN-viral DNA complex) and ternary (IN-viral DNA- INSTI) IN flexibility. RMSD analyses revealed that that the mutants have a rigid structure relative to the WT IN. Furthermore, mutant IN showed transient changes in the secondary structure of the 140s loop compared to the WT. In addition to these reduced flexibility and structural changes, resistance mutations alter the binding mode of RAL, ELV, and DTG to IN and viral DNA. This study is the first to identify a structural basis of IN mechanism of resistance to INSTI's resistance that develops under treatment pressure in HIV-1 IN.

AUTOBIOGRAPHICAL STATEMENT

Education

Master of Science in Biochemistry and Molecular Biology   December 2015
Wayne State University School of Medicine, Detroit, MI   **GPA:** 3.7/4.0

Bachelor of Science in General Biology   May 2012
Kentucky State University, Frankfort, KY   **GPA**: 3.1/4.0

Publications

Antonious, G.; Hill, R.; **Ross, K**.; Coolong, T. Dissipation, half-lives, and mass spectrometric of endosulfan isomers and the sulfate metabolites on three field-grown vegetables. *J Environ Sci Health B* 2012, 47, 369-78.

Chorida P, Dewdney TG, Keusch B, Kuiper BD, **Ross K**, Kovari IA, MacArthur R, Salimnia H, Kovari LC. The role of mutations at codons 32, 47, 54, and 90 in HIV-1 protease flap dynamics, Discoveries 2014, Oct- Dec; 2(4):e27.

Manuscripts in Preparation

Ross, K., Keusch, Kuiper, B., Kovari, I.A., and Kovari L.C. **(2015).** *A comprehensive review of HIV-integrase inhibitors 2007-2015.* Manuscript in preparation.

Ross, K., Dewdney, T. G., Kuiper, B. D., Keusch, B., Kovari, I. A., and Kovari L. C. **(2015).** *Reduced HIV-1 integrase flexibility correlates with raltegravir, elvitegravir, and dolutegravir HIV-1 integrase resistance*. Manuscript in preparation.

Ross, K. (2015). *Molecular Dynamic Studies of HIV Integrase Mechanisms of Resistance to Elvitegravir and Dolutegravir.* MS Thesis. Wayne State University School of Medicine: USA. Manuscript in preparation.

Kuiper, B. D., Keusch, B., Dewdney, T., Chordia, P., **Ross, K.,** Kovari, I. A., Kovari, L. C. **(2015).** *The L33F darunavir resistance mutation acts as a molecular anchor reducing the flexibility of the HIV-1 protease 30's and 80's loops.* Manuscript in preparation.

Achievements
- Kentucky Academy of Science- 2010 first place award
- Kentucky Academy of Science- 2011 Second Place
- Associates of Research Directors Symposium 2010
- American Association for University Women 2011
- L-SAMP Symposium -2011 Second place award
- National Conference for Undergraduate Research Showcase 2012
- Wayne State University BMB Department Scholarship award winner 2014-2015